JOURNAL OF AGRICULTURAL AND FOOD CHEMISTRY

pubs.acs.org/JAFC Article

Differential Morpho-Physiological, Ionomic, and Phytohormone Profiles, and Genome-Wide Expression Profiling Involving the Tolerance of Allohexaploid Wheat (*Triticum aestivum* L.) to Nitrogen Limitation

Qiong Li, Hai-li Song, Ting Zhou, Min-nan Pei, Bing Wang, Song-xian Yan, Yun-qi Liu, Peng-jia Wu,* and Ying-peng Hua*

Cite This: *J. Agric. Food Chem.* 2024, 72, 3814−3831 Read Online

ACCESS | Metrics & More | Article Recommendations | Supporting Information

ABSTRACT: Common wheat (*Triticum aestivum* L.) is a global staple food, while nitrogen (N) limitation severely hinders plant growth, seed yield, and grain quality of wheat. Genetic variations in the responses to low N stresses among allohexaploid wheat (AABBDD, $2n = 6x = 42$) genotypes emphasize the complicated regulatory mechanisms underlying low N tolerance and N use efficiency (NUE). In this study, hydroponic culture, inductively coupled plasma mass spectrometry, noninvasive microtest, high-performance liquid chromatography, RNA-seq, and bioinformatics were used to determine the differential growth performance, ionome and phytohormone profiles, and genome-wide expression profiling of wheat plants grown under high N and low N conditions. Transcriptional profiling of NPFs, NRT2s, CLCs, SLACs/SLAHs, AAPs, UPSs, NIAs, and GSs characterized the core members, such as *TaNPF6.3-6D*, *TaNRT2.3−3D*, *TaNIA1−6B*, *TaGLN1;2−4B*, *TaAAP14−5A/5D*, and *TaUPS2−5A*, involved in the efficient transport and assimilation of nitrate and organic N nutrients. The low-N-sensitivity wheat cultivar XM26 showed obvious leaf chlorosis and accumulated higher levels of ABA, JA, and SA than the low-N-tolerant ZM578 under N limitation. The TaMYB59−3D-*TaNPF7.3/NRT1.5−6D* module-mediated shoot-to-root translocation and leaf remobilization of nitrate was proposed as an important pathway regulating the differential responses between ZM578 and XM26 to low N. This study provides some elite candidate genes for the selection and breeding of wheat germplasms with low N tolerance and high NUE.

KEYWORDS: *genotypic difference, nitrogen limitation, multiomics, transporter, wheat*

INTRODUCTION

Nitrogen (N) deficiency in soils is a major constraint on crop production and yield, and the consumption of N fertilizers accounts for approximately 60% of the total fertilizers used in agriculture annually.[1] The application of N fertilizers not only enhances yield but causes environmental pollution and resource wastage.[2] Crop N use efficiency (NUE) involves the processes of N uptake, translocation, assimilation, compartmentation, and remobilization.[2] Comprehensive studies of the genetic and molecular mechanisms underlying crop NUE regulation are crucial for enhancing crop NUE and breeding N-efficient crop germplasms.

Wheat is one of the most important food crops, providing about 40% of food demand for the world's population.[3] The application of N fertilizers plays an indispensable role in regulating wheat seed yield and grain protein content.[4] Although substantial progress has recently been made in exploring efficient N use strategies in major crops, the NUE of wheat remains significantly lower than those of maize and rice.[5,6] Common wheat is an allohexaploid crop species comprising subgenomes A, B, and D subgenomes. It originated from two successive rounds of polyploidization within the genera *Triticum* and *Aegilops*, forming tetraploid wheat (AABB) and hexaploid wheat (AABBDD, $2n = 6x = 42$), respectively.[7] Previous studies on the genes controlling NUE have been conducted in model plants *Arabidopsis* and rice. However, the pivotal mechanisms underlying high NUE and core regulatory genes have not been well elucidated and characterized in allohexaploid wheat with huge and complicated genomes,[8] which pose great challenges to improve the wheat NUE. Therefore, unraveling the core gene(s) governing NUE and characterizing the elite genetic alleles among natural population is an important prerequisite for the breeding of N-efficient wheat cultivars.

Nitrate (NO_3^-) is a major form of N nutrient absorbed by the roots of upland crop species, such as common wheat. Four types of nitrate transporters, namely, low-affinity nitrate transporter 1 (NRT1s) or nitrate/peptide families (NPFs), high-affinity nitrate transporters 2 (NRT2s) coupled with nitrate assimilation related 2s (NAR2s/NRT3.1s), slow-type anion channels (SLACs/SLAH), and chloride channels (CLCs), are responsible for efficient N uptake and transport.[9] Following N uptake, either the inorganic N is assimilated into amino acids in roots

Received: November 19, 2023
Revised: January 9, 2024
Accepted: January 25, 2024
Published: February 8, 2024

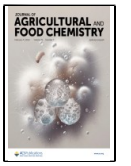

https://doi.org/10.1021/acs.jafc.3c08626
J. Agric. Food Chem. 2024, 72, 3814−3831

and translocated through the xylem to the shoots or NO_3^- is allocated with transpiration streams to leaves where the assimilation occurs.[10] Intensive leaf N metabolism, including proteolysis and N reassimilation, also occurs during grain development.[13] Loading of organic N compounds into leaf phloem is generally undertaken by amino acid, peptide, and oligopeptide transporters.[14] In wheat grains, >75% of the N/proteins may be derived from remobilization in vegetative organs.[15] Leaves are the major sources for N (re)distribution to grains, especially flag leaves, which display high longevity[11] and contribute ca. 18−24% of the total grain N content.[16] At preanthesis, considerable N assimilates may be used for leaf metabolism or transient storage,[11] while at postanthesis, the majority of newly synthesized amino acids may be loaded into leaf phloem to supply N nutrients for growing wheat grains.[12] Nitrate reductase (NR), glutamine synthetase (GS), and glutamine synthase (GOGAT) are key enzymes in primary N assimilation.[17] Besides the transporters and enzymes, many transcription factors have also been identified as pivotal regulators involved in plant N responses.[9,18,19] Thus, understanding the gene networks governing N uptake, remobilization, and assimilation will facilitate the design of wheat cultivars with improved yields, NUE, and grain protein content.

Moderately low N enhances crop NUE;[20] therefore, improving crop tolerance to low N is highly significant for the NUE enhancement. Based on the argument above, in this study, we were aimed to (i) explore the morpho-physiological changes of wheat under N limitation, (ii) screen the core differentially expressed genes (DEGs) from the wheat transcriptome responsive to low N, and (iii) uncover the key regulatory mechanisms and core genes in different wheat genotypes with differential low N tolerance and NUE. The findings of this study will provide some elite candidate genes for the selection and breeding of wheat germplasm with low N tolerance and high NUE.

MATERIAL AND METHODS

Plant Materials and Growth Conditions. Wheat seedlings of similar sizes after the germination of 0.5% (w/v) NaClO-sterilized seed were transplanted into black plastic containers with full-strength Hoagland and Arnon solution.[21] Wheat plants were grown in an artificial climate chamber with a temperature regime of 24:22 °C (day/night), a photoperiod of 14:10 h (day/night), and a light intensity of 300−320 μmol m^{-2} s^{-1}. To identify the core N transporter genes, uniform wheat seedlings (cv. Chinese Spring) were hydroponically grown under high N (6.0 mM NO_3^-) and low N (0.30 mM NO_3^-) conditions for 20 days until sampling for physiological and transcriptomic analysis. To reveal the physiological and transcriptional differences in low N tolerance between wheat genotypes, uniform wheat seedlings of Zhongmai 578 (ZM578, developed by the Chinese Academy of Agricultural Sciences) and Xinmai 26 (XM26, developed by Xinxiang Academy of Agricultural Sciences), selected as a low-N-tolerant cultivar and a low-N-sensitive cultivar, respectively, were hydroponically grown under high N (6.0 mM NO_3^-) and low N (0.30 mM NO_3^-) conditions for 20 days until sampling for comparative physiological and transcriptomic analysis.

Determination of Root System Architecture. The roots of wheat plants (cv. Chinese Spring, ZM578, and XM26), which were hydroponically grown under high N (6.0 mM NO_3^-) and low N (0.30 mM NO_3^-) conditions for 20 days, were imaged using a scanner (Epson Perfection V800 photo, Epson, Suwa, Japan). The root system architecture parameters, including total root length, root surface area, average root diameter, total root volume, and root tip number, were analyzed using the WinRHIZO2003b software. Each measurement was conducted with five independent biological replicates.

Ionome Determination. The dried shoot and root samples (about 0.1 g) of wheat plants (cv. Chinese Spring, ZM578, and XM26), hydroponically grown under high N (6.0 mM NO_3^-) and low N (0.30 mM NO_3^-) conditions for 20 days, were digested in conical flasks with 10 mL of a mixture of acid ($HClO_4/HNO_3$ = 1:3, v/v). The concentrations of K, Ca, Mg, Na, Fe, Mn, Cu, and Zn in the shoots and roots were determined by an inductively coupled plasma-optical emission spectrometer (Agilent ICAP 7000, Palo Alto, California).

Measurement of NO_3^-, K^+, and Ca^{2+} Fluxes Using Noninvasive Microtest. In the roots of wheat plants (cv. Chinese Spring) hydroponically grown under high N (6.0 mM NO_3^-) and low N (0.30 mM NO_3^-) conditions for 20 days, NO_3^-, K^+, and Ca^{2+} fluxes were measured using noninvasive microtest (Xuyue, Beijing, China). The preparation and calibration of the ion microsensors were performed according to our previous work.[23] The roots were immersed in the measuring solution (0.1 mM KCl, 0.1 mM $CaCl_2$, 0.1 mM $MgCl_2$, 0.5 mM NaCl, 0.2 mM Na_2SO_4, and 0.3 mM MES; pH 5.7). The measuring chamber was mounted on a microrobotic arm with electrodes near the root surface. The measurement of the gradient of NO_3^-, K^+, Ca^{2+}, and H^+ adjacent to the roots was measured by employing a selective microelectrode for NO_3^-, K^+, Ca^{2+}, and H^+, which was moved between two predetermined sites with offsets of 30 and 10 μm, correspondingly. The fluxes of NO_3^-, K^+, Ca^{2+}, and H^+ were recorded for 5 min. All of the experiments were performed with at least eight biological replicates.

Determination of Total N and NO_3^- Concentration. Wheat plants (cv ZM578 and XM26) were hydroponically grown under high N (6.0 mM NO_3^-) and low N (0.30 mM NO_3^-) conditions for 20 days until sampling. The shoot and root samples were ground in liquid nitrogen and placed in a shaker mill with distilled water, and then, NO_3^- was extracted. The concentrations of NO_3^- and total N were measured using the salicylic acid method.[16,24]

Phytohormone Analysis. Fresh shoot and root samples (~0.5 g) of wheat plants (cv. ZM578 and XM26), hydroponically grown under high N (6.0 mM NO_3^-) and low N (0.30 mM NO_3^-) conditions for 20 days, were lyophilized. Extraction liquid (80% methanol: 0.5% formic acid; 1:1, v/v) was added, soaked overnight, shaken, and centrifuged to obtain the supernatant. The solid phase extraction column was activated and balanced with 5 mL methanol and 5 mL water, and then the extraction solution was processed in the column. Subsequently, the column was washed with 15% methanol and eluted with 5 mL of methanol. The eluent was collected. The eluent was blown dry with N_2 and redissolved in 1 mL of 20% methanol. Finally, the extract was centrifuged, and the supernatant concentration was measured. The concentrations of salicylic acid (SA), jasmonic acid (JA), abscisic acid (ABA), gibberellin (GA_3/GA_7), indole-3-acetic acid (IAA), brassinolide (BR), *trans*-zeatin (*t*Z), *cis*-zeatin (*c*Z), *trans*-zeatin-riboside (*t*ZR), and N6-(delta 2-isopentenyl)-adenine (2-iPA) were detected using an ultrahigh-performance liquid chromatography−triple quadrupole series mass spectrometer (QTrap6500, SCICEX, Boston, Massachusetts). All of the experiments were performed with three biological replicates.

High-Throughput RNA-seq. The shoots and roots of wheat seedlings (cv. Chinese Spring, ZM578, and XM26) were individually sampled and were subjected to mRNA sequencing (RNA-seq). Total RNA was extracted using TRIzol (Invitrogen, Life Technologies, Carlsbad, California), and gDNA was removed using DNase I (TaKaRa, Otsu, Shiga, Japan). RNA quality and quantity were assessed using a 2100 Bioanalyser (Agilent, California) and a NanoDrop 2000 (Thermo Fisher Scientific, Waltham, Massachusetts), respectively. For each sample, 150 bp paired-end reads were generated by using the Illumina HiSeq X Ten platform (Illumina Inc., San Diego, California). Analysis of RNA-seq data, including identification of DEGs and Gene Ontology (GO) and Kyoto Encyclopedia of Genes and Genomes (KEGG) analysis, followed our previously published studies.[22] A false discovery rate (FDR) of $\leq$0.05 and $\log_2$(fold-change) of $\geq$1.0 were used as the thresholds to identify the DEGs.

Reverse-Transcription Quantitative PCR Assays. Reverse-transcription quantitative PCR (RT-qPCR) assays were performed to determine the expression patterns of target genes under different nutrient stresses. For the low-K treatment, the wheat plants (cv Chinese

https://doi.org/10.1021/acs.jafc.3c08626
J. Agric. Food Chem. 2024, 72, 3814−3831

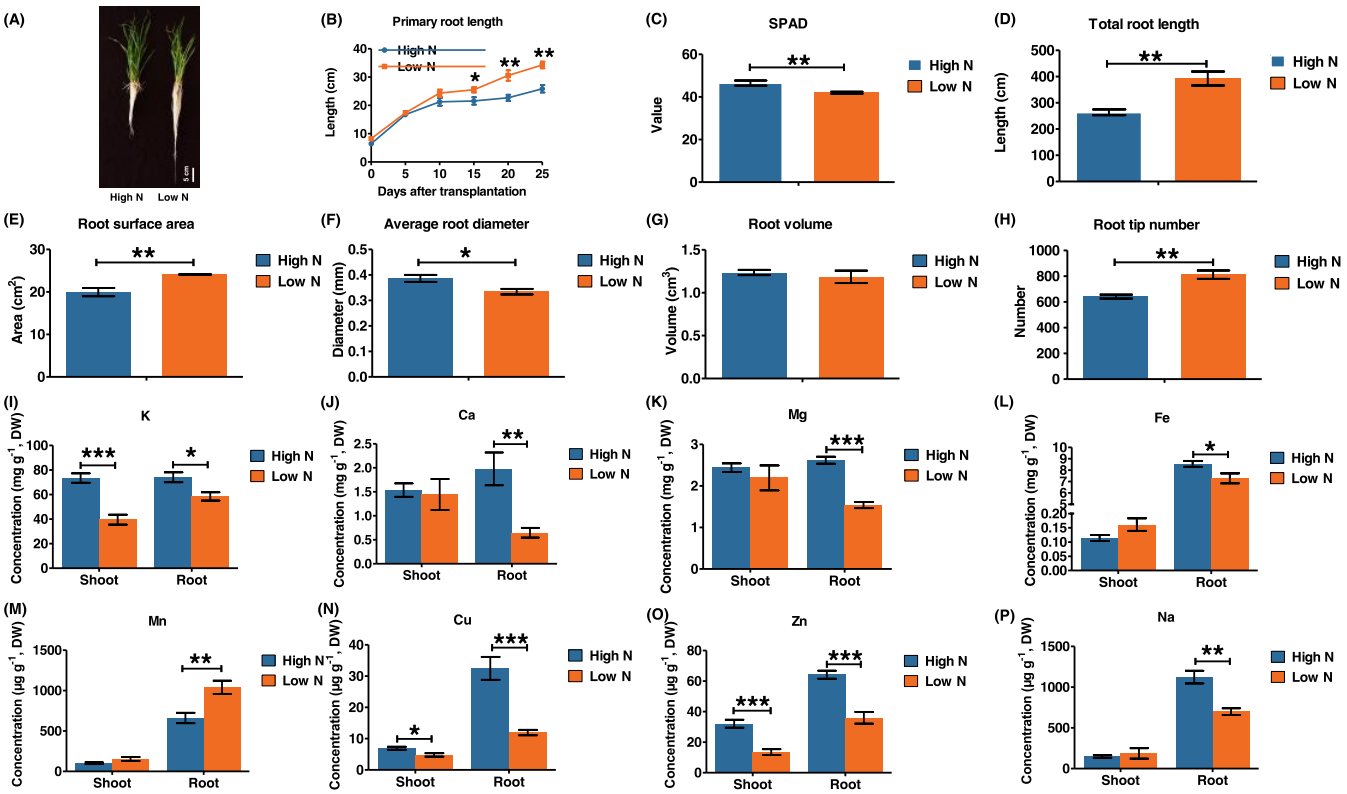

Figure 1. Growth performance, root system architecture, and ionomic profiling of wheat plants under high N and low N conditions. (A−H) Growth performance (A), dynamic primary root growth status (B), SPAD values (C), total root length (D), root surface area (E), average root diameter (F), root volume (G), and root tip number (H) of wheat plants (cv. Chinese Spring) grown under high N and low N conditions. (I−O) The concentrations of K (I), Ca (J), Mg (K), Fe (L), Mn (M), Cu (N), Zn (O), and Na (P) of wheat plants grown under high N and low N conditions. Uniform wheat seedlings (cv. Chinese Spring) were hydroponically grown under high N (6.0 mM NO_3^-) and low N (0.30 mM NO_3^-) conditions for 20 days until sampling. Data are presented as mean ($n = 5$) ± s.d. Significant differences (*$p < 0.05$; **$p < 0.01$; ***$p < 0.001$) were determined by unpaired two-tailed Student's t tests between two groups using the SPSS 17.0 toolkit.

Spring) were grown under high K/control (6.0 mM) and low K (0.05 mM) for 20 days until the roots were sampled. Regarding the low-Fe treatment, the wheat plants were grown under high Fe/control (50 μM EDTA-Fe) and low Fe (2.0 μM EDTA-Fe) for 20 days until the roots were sampled individually. In the salt stress treatment, the wheat plants were grown under control (salt-free) and salt stress (100 mM NaCl) conditions for 20 days until the roots were sampled individually. For the saline-alkaline stress treatment, the wheat plants were grown under control (salt-free) and saline-alkaline (75 mM $NaHCO_3$) conditions for 20 days until the roots were sampled individually.

Following treatment of RNA samples, isolated by prechilled Trizol with RNase-free and DNase I, the gDNA Eraser Takara PrimeScript RT Reagent Kit was utilized to synthesize cDNA using total RNA as templates. SYBR Premix Ex *Taq*II (TaKaRa, Shiga, Japan) was used for RT-qPCR amplification, which was run on an Applied Biosystems StepOne Plus Real-time PCR System (Thermo Fisher Scientific, Waltham, Massachusetts). The thermal cycles were as follows: 95 °C for 3 min, followed by 40 cycles of 95 °C for 10 s and 60 °C for 30 s. The following protocol was used to plot the melting curve: 95 °C for 15 s, 60 °C for 1 min, and 60−95 °C for 15 s (+0.3 °C per cycle). Two public reference genes, *TaGAPDH-7B* (TraesCS7B02G213300) and *TaActin-1A* (TraesCS1A02G274400), were used to normalize the expression data,[25] and the $2^{-\Delta\Delta CT}$ method was used to normalize relative gene expression.[26]

Molecular Characterization of Target Gene(s). The physicochemical parameters of the target protein were calculated using PROTPARAM (http://web. expasy.org/protparam/), and the hydrophobicity was plotted using DNASTAR (http://www.dnastar.com/). Transmembrane helices of the target protein were predicted by using the TMHMM Server (http://www.cbs.dtu.dk/services/TMHMM-2.0/). Expression profiling of the target gene(s) was retrieved from the wheat eFP browser (https://bar.utoronto.ca/efp_wheat/cgibin/efpWeb.cgi). Analysis of the transcriptional regulatory network was performed in the wGRN database (http://wheat.cau.edu.cn/wGRN/).

Subcellular localization of the target gene(s) was determined using poly(ethylene glycol)-mediated protoplast transformation in rice, and rice MCA1 was used as a plasma membrane marker with red fluorescence. Fluorescence was observed using a Nikon C2-ER confocal laser-scanning microscope with emission filters set at 510 nm (GFP) and 580 nm (RFP), and excitation was achieved at 488 nm (GFP) and 561 nm (RFP).

Statistical Analysis. For statistical testing, Student's t tests and one-way analysis of variance (ANOVA) were used to determine significant differences, followed by Tukey's honestly significant difference multiple comparison tests using SPSS 17.0 (Chicago, Illinois).

Data Availability. All of the data supporting the findings of this study are available within the paper and within its Supporting Data published online. The raw data of the high-throughput transcriptome sequencing have been deposited in the NCBI Sequence Read Archive (SRA) under the Bioproject accession no. PRJNA985048.

RESULTS

Morpho-Physiological Responses of Allohexaploid Wheat Plants to N Deficiency. The physiological responses of Chinese Spring to N limitation were determined by hydroponically growing the plants under high (6.0 mM) and low (0.30 mM) NO_3^- conditions. After 20 days of plant growth, the long-term N limitation significantly affected the shoot and root growth of Chinese Spring (Figure 1A). Low N induced the elongation of the primary roots of Chinese Spring (Figure 1B),

https://doi.org/10.1021/acs.jafc.3c08626
J. Agric. Food Chem. 2024, 72, 3814−3831

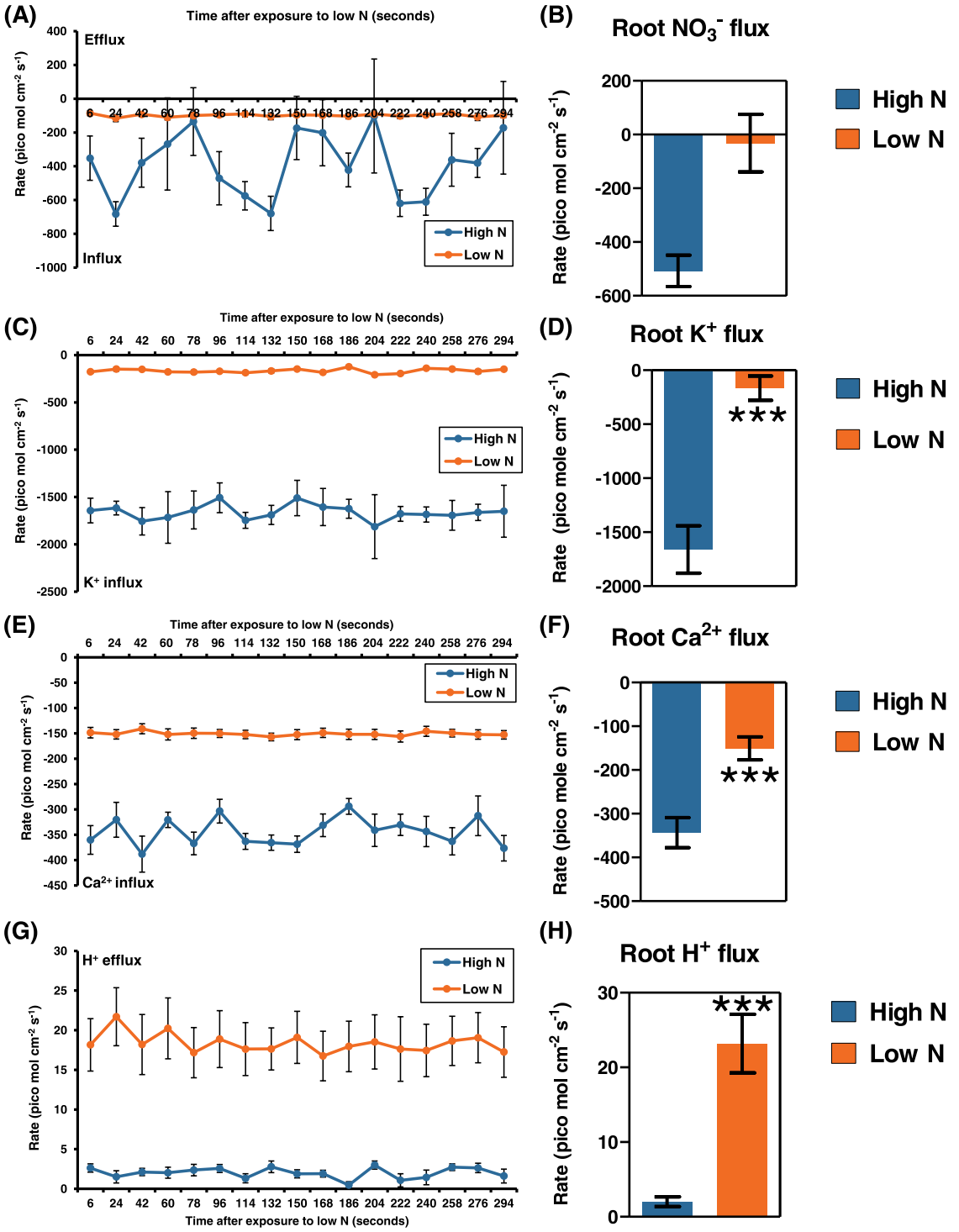

Figure 2. Dynamic and net flux rate of NO_3^- combined with K^+, Ca^{2+}, and H^+ in the primary roots of wheat seedling grown under high N and low N conditions. Dynamic flux rate and net flux rate of NO_3^- (A, B), K^+ (C, D), Ca^{2+} (E, F), and H^+ (G, H). The positive and negative data indicate the efflux and influx rates of ions, respectively. Data are presented as mean (n = 8) ± s.d. Significant differences (*p < 0.05; **p < 0.01; ***p < 0.001) were determined by unpaired two-tailed Student's t tests between two groups using the SPSS 17.0 toolkit.

while the leaves became severely chlorotic, which was indicated by the obviously reduced SPAD values (Figure 1C). The total root length (Figure 1D), root surface area (Figure 1E), and root tip number (Figure 1H) of Chinese Spring were significantly increased under low N compared with high N conditions. However, the average root diameters of Chinese Spring were decreased under low N than under high N conditions (Figure 1F), while the root volumes were not significantly changed between the two N levels (Figure 1G). Furthermore, we also tested the concentration profiling of several metal ions, including K, Ca, Mg, Fe, Mn, Cu, Zn, and Na, to explore the N-induced growth changes (Figure 1I–P). In total, the concentrations of these cations were significantly altered in the wheat plants grown under low N compared with those grown under high N (Figure 1I–P). In detail, in the shoots, the concentrations of K, Cu, and Zn were significantly reduced

https://doi.org/10.1021/acs.jafc.3c08626
J. Agric. Food Chem. 2024, 72, 3814−3831

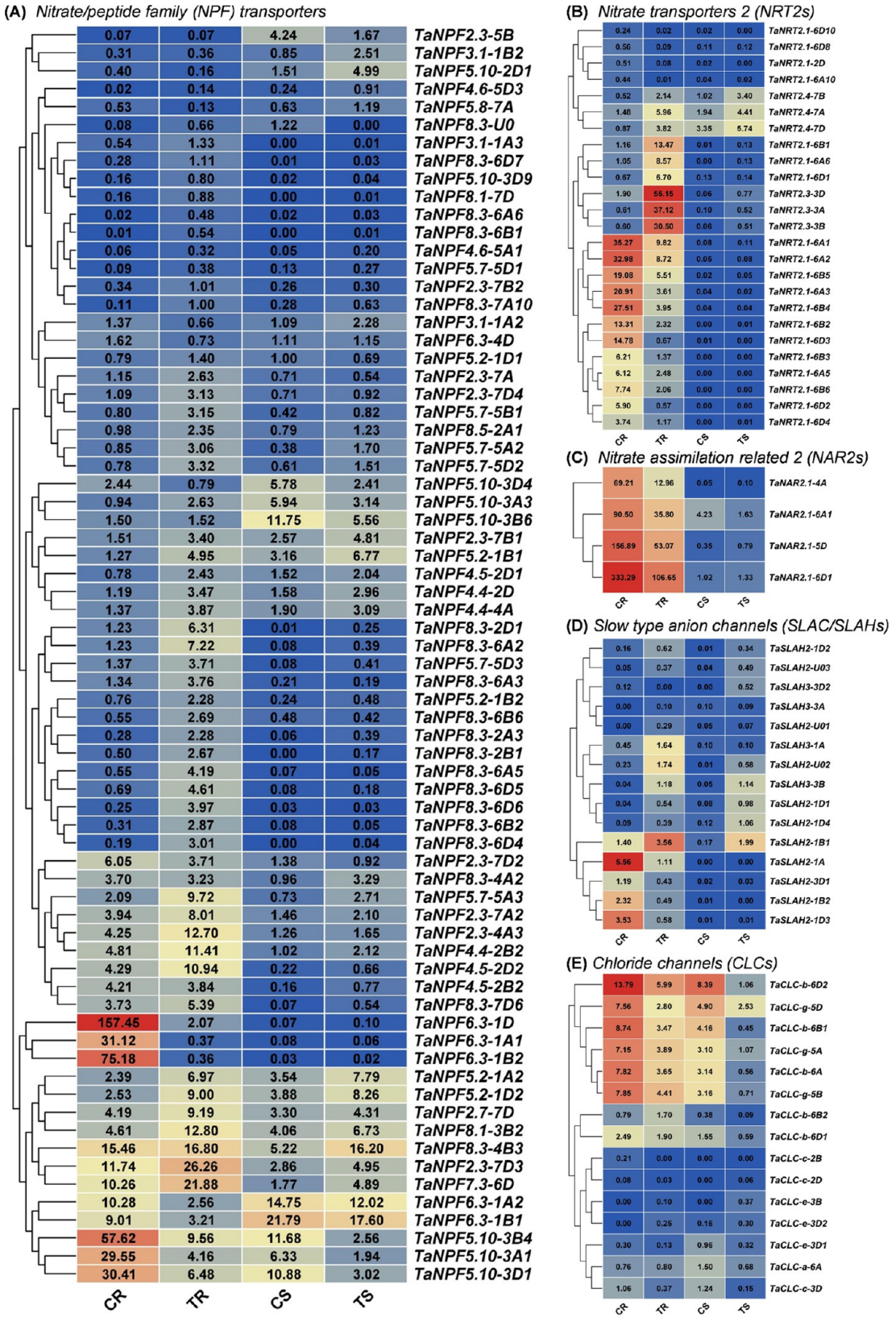

Figure 3. Differential expression analysis of some nitrate transporter genes in the shoots and roots of wheat plants grown under high nitrogen (N) and low N conditions. (A–E) Differential gene expression of the (A) nitrate/peptide family (NPF), (B) nitrate transporter 2 (NRT2), (C) nitrate assimilation related 2 (NAR2), (D) slow-type anion channel (SLAC/SLAH), and (E) chloride channel (CLC) in the shoots and roots of wheat plants grown under high N and low N conditions. Regarding the RNA-seq experiment, the wheat plants (cv. Chinese Spring) that were grown under high N (6.0 mM NO_3^-) and low N (0.30 mM NO_3^-) for 20 days until the shoots and roots were individually sampled. False discovery rate (FDR) ≤ 0.05 and $\log_2$ (fold-change) ≥ 1.0 are used as the thresholds to identify DEGs. C, control (high N); T, treatment (low N); S, shoot; R, root.

https://doi.org/10.1021/acs.jafc.3c08626
J. Agric. Food Chem. 2024, 72, 3814–3831

under N deficiency while obvious differences were not detected in the concentrations of the other cations. In the roots, except for the Mn concentrations were markedly reduced, the concentrations of the other cations (namely, K, Ca, Mg, Fe, Cu, Zn, and Na) were significantly increased under low N conditions.

To determine the effect of low NO_3^- condition on the dynamic flux of other ions, the net influxes of NO_3^- combined with H^+, K^+, and Ca^{2+} in the primary roots of Chinese Spring were measured using the noninvasive microtest technology. The results showed that a stronger NO_3^- influx rate was identified in the roots of wheat plants grown under high N than under low N (Figure 2A,B). Moreover, we found that the NO_3^- influx showed more obvious periodic fluctuation in Chinese Spring grown under high N than under low N (Figure 2A,B). The two cation rates of both dynamic and net flux were significantly smaller under low N than under high N (Figure 2C−F), which is consistent with the results of reduced K and Ca concentrations in the roots of Chinese Spring (Figure 1I,J). The flux of NO_3^- is driven by the H^+ gradient across the plasma membrane;[27] under low N, we found a greater increase in the H^+ efflux in the roots of Chinese Spring compared with those under high N (Figure 2G,H).

Genome-Wide Transcriptional Responses of Allohexaploid Wheat Plants to N Limitations. After discarding adapter sequences and low-quality reads, on average, approximately 4.9×10^7 clean reads were obtained for each sample, and the total length of clean reads reached about 8.5×10^{10} nt with Q_{20} > 97% and Q_{30} > 92% (Table S1). In general, the GC content of the 12 RNA samples from wheat plants was about 58% (Table S1). For each sample, ∼94% of the clean reads were mapped to the reference transcriptome sequence of Chinese Spring (Table S1).

In total, the shoots and roots of Chinese Spring exhibited significantly differential transcriptomic features under high and low N conditions (Figure S2A), indicating N-level-dependent transcriptional responses. Most of the Pearson correlation coefficients were more than 0.95 between each pair of biological replicates (Figure S2B). Ten DEGs were randomly selected to compare their expression consistency between the RT-qPCR assays and transcriptome sequencing. The expression of most genes was highly correlated (r > 0.99) between the two assays (Figure S1); both of these results indicated that the mRNA sequencing data were of good quality. In general, 6696 and 8537 genes were identified to be differentially expressed in the shoots and roots, respectively (Figure S2C). An intersection analysis presented by a Venn diagram indicated that 1751 DEGs were detected simultaneously in both shoots and roots (Figure S2C).

In both the shoots and roots of Chinese Spring, the highly enriched GO terms were mainly related to nitrate transport and metabolism and responses to phytohormones, including JA, GA, and SA (Figure S3A,B). Consistently, photosynthesis in the shoots and phenylpropanoid biosynthesis in the roots were the most active KEGG pathways (Figure S4A,B), while the N metabolism pathway was commonly identified to be highly overrepresented in both shoots and roots (Figure S4A,B).

Transcriptional Characterization of the Core Genes Associated with N Transport and Metabolism to N Limitations. A total of 53 *NRT1s/NPFs*, 7 *NRT2s*, 5 *SLACs/SLAH*, and 7 *CLCs* have been annotated in the *Arabidopsis* genome; these transporters expanded hugely in crop species,[28−31] particularly those with complex and large genomes (such as oilseed rape and common wheat). However, prior to this study, the core N transporter genes remained unknown in allohexaploid wheat. Through characterizing the transcriptional profiling of the nitrate transporter genes (Table S2), we found that different members showed remarkable differences in their expression patterns, including expression tissues and abundances in Chinese Spring grown under high N and low N conditions (Figure 3). Among the differentially expressed *TaNPF* members, several *NPF6.3* homologues showed the highest expression levels; they were mainly expressed in the roots and presented higher transcriptional abundances under high N than under low N (Figure 3A), indicating their low affinity for NO_3^- transport under high N condition. In general, all *TaNRT2s* were mainly expressed in the roots; among them, the expression of three *NRT2.3* homologues (*TaNRT2.3A/B/D*) was significantly upregulated under low N and showed the highest expression levels (Figure 3B). Among the four *TaNAR2* DEGs, all of them were downregulated under low N concentrations (Figure 3C). Different *TaSLAC/SLAH* members showed differential responses to low N, and *TaSLAH2-1A* expression was induced by low N, which repressed *TaSLAH2-1B1* expression (Figure 3D). Among the *CLC* homologues, *TaCLCb-6D2* showed the highest transcriptional abundance in both shoots and roots, and was induced by high N (Figure 3E).

Subsequently, we investigated the differential expression profile and core members of some key N assimilation, organic N transporter, and NUE-regulatory genes (Table S2; Figure 4). All *nitrate reductase* (*NIA*) genes were significantly induced by high N, and *TaNIA1-6B* presented the highest transcript level (Figure 4A). The *glutamine synthetase* (*GLN*) genes consisted of two subgroups: *GLN1* and *GLN2*, which showed obviously distinct tissue-specific expression patterns. *TaGLN 1s* and *TaGLN 2s* were mainly expressed in the roots and shoots, respectively. However, the *TaGLN* DEGs were induced by high N (Figure 4B). Organic N nutrients are major sources for N remobilization in plants; in cereals, 50−90% of seed N is derived from remobilized N nutrients.[32] Therefore, we paid more attention to the organic N transporter genes induced by low N, which had a higher NUE than high N.[20] In terms of the *amino acid permease* (*AAP*) genes, most of the DEGs were upregulated in shoots and roots under low N concentrations (Figure 4C). In the shoots, *TaAPP 2s*, *TaAPP12s*, and *TaAPP14s* showed relatively higher expression levels than other members; in the roots, the expression of *TaAPP 2s*, *TaAPP14s*, and *TaAPP15s* was higher than that of the other *AAP* homologues (Figure 4C). Overexpression of ureide permease (UPS), which moves allantoin/allantoate from roots to source leaves to sink leaves, can lead to improved seed yield and protein content.[33,34] The *UPS1* and *UPS2* subgroups showed differential expression preferences and transcriptional responses to low N content (Figure 4D). *TaUPS 1s* were mainly expressed in the roots while *TaUPS 2s* did not show an obviously distinct expression preference; *TaUPS 1s* and *TaUPS 2s* were downregulated and upregulated under low N, respectively (Figure 4D). In terms of other organic N transporter genes, although *TaATLa 5s* had the highest transcriptional abundance, their expression was repressed by low N (Figure 4E). In general, the *TaLHT* genes not only had moderately higher expression levels but also were upregulated under low N (Figure 4E). In addition, we also investigated the expression of two other family genes, including *autophagy-related genes* (*ATGs*) and E3 ubiquitin ligase genes (*NLAs*) (Figure 4F,G). It was noteworthy that the expression of *TaATGs* was obviously induced by low N concentration in the shoots (Figure 4F), and their increased expression might contribute to efficient N recycling. However, *TaNLAs* were

https://doi.org/10.1021/acs.jafc.3c08626
J. Agric. Food Chem. 2024, 72, 3814−3831

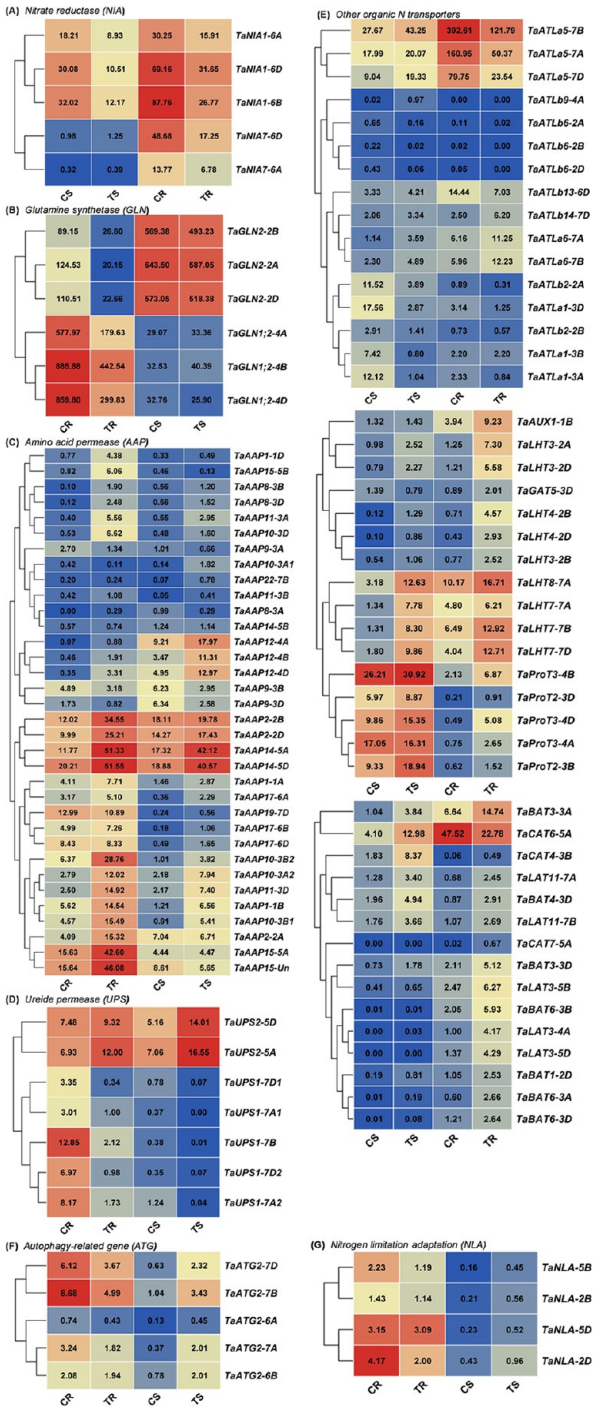

Figure 4. Differential expression analysis of some nitrogen (N) assimilation genes, organic N transporter genes, and key NUE-regulatory genes in the shoots and roots of wheat plants grown under high N and low N conditions. (A−E) Differential gene expression of the (A) nitrate reductase (NIA), (B) glutamine synthetase (GLN), (C) amino acid permease (AAP), (D) ureide permease (UPS), (E) other organic N transporters, (F) autophagy-related gene (ATG), and (G) nitrogen limitation adaptation (NLA) genes in the shoots and roots of wheat plants grown under high N and low N conditions. Regarding the RNA-seq experiment, the wheat plants (cv. Chinese Spring) that were grown under high N (6.0 mM NO_3^-) and low N (0.30 mM NO_3^-) for 20 days until the shoots and roots were individually sampled. False discovery rate (FDR) ≤ 0.05 and $\log_2$ (fold-change) ≥ 1.0 are used as the thresholds to identify DEGs. C, control (high N); T, treatment (low N); S, shoot; R, root.

downregulated in the roots under low N (Figure 4G), and their downregulation might facilitate enhanced root-to-shoot N translocation under low N.

Taken together, genome-wide differential expression profiling provided valuable information for the selection of candidate elite genes for the genetic improvement of efficient N use in allohexaploid wheat through the molecular modification of these genes.

Differential Morpho-Physiological Responses to N Deficiency between the Low-N-Tolerant and Low-N-Sensitive Wheat Genotypes. Moderately low N condition improves NUE in crops;[20] therefore, promoting low N tolerance is greatly important for the NUE enhancement. However, significant genotypic diversity in response to low N stresses was identified among different wheat genotypes.[6] In this study, we found that under high N, the low-N-tolerant wheat cultivar ZM578 and the low-N-sensitive wheat cultivar XM26 did not show obvious differences in the growth performance of either shoots or roots; however, XM26 showed remarkable chlorosis in the old leaves compared with ZM578, which presented much stronger roots (Figure 5A,B). Specifically, the values of leaf SPAD and the maximal root length of ZM578 were significantly higher than those of XM26 under N limitation (Figure 5C,D). To specify the detailed physiological reasons for the differential N limitation tolerance between ZM578 and XM26, we first determined the concentrations of total N and NO_3^- in the shoots and roots. The results showed that the total N concentrations of shoots and roots did not differ between the two wheat genotypes (Figure 5E,F), which indicated that N uptake was not involved in the differential N tolerance between the two wheat genotypes. Moreover, the ratio of $root_{[total\ N]}$/$shoot_{[total\ N]}$ was also highly similar between ZM578 and XM26 (Figure 5G). Subsequently, we tested the NO_3^- concentrations; under low N, the root NO_3^- concentration was significantly higher in XM26 than in ZM578 (Figure 5I), while the shoot concentrations did not differ between the two cultivars (Figure 5H). Furthermore, the low-N-tolerant cultivar ZM578 had a lower ratio of $root_{[total\ NO_3^-]}$/$shoot_{[total\ NO_3^-]}$ than XM26 (Figure 5J), which indicated a higher proportion of long-distance NO_3^- translocation from roots to shoots in ZM578. In addition, we found that the concentrations of shoot Ca/Zn and root Fe were significantly higher in XM26 than in ZM578, while the concentrations of other cations in the shoots or roots were not different between the two cultivars (Figure 5K−R).

Differential Gene Expression Profiling between the Low-N-Tolerant and Low-N-Sensitive Wheat Genotypes. To explore the potential molecular mechanisms underlying differential low N tolerance, an Illumina HiSeq 4000 system was used to perform high-throughput transcriptional profiling of the low N tolerance ZM578 and the low-N-sensitive XM26. After removal of adaptor sequences and low-quality reads, more than 4.7×10^7 clean reads, on average, were obtained for each sample, and the total length of clean reads reached 1.3×10^{10} nt with a base-calling accuracy of more than 98% of Q_{20} and 95% of Q_{30} (Table S3). In general, the GC contents of 24 RNA samples of ZM578 and XM26 were about 55% in this study. For each sample, ∼90% of the clean reads were mapped onto the reference transcriptome sequence of Chinese Spring.

A total of 30 647 and 31 107 DEGs were identified in the shoots and roots of ZM578 and XM26 grown under low N (Figure 6A). A Venn diagram-mediated intersection analysis was performed to identify the genes specifically responsive to low N;

https://doi.org/10.1021/acs.jafc.3c08626
J. Agric. Food Chem. 2024, 72, 3814−3831

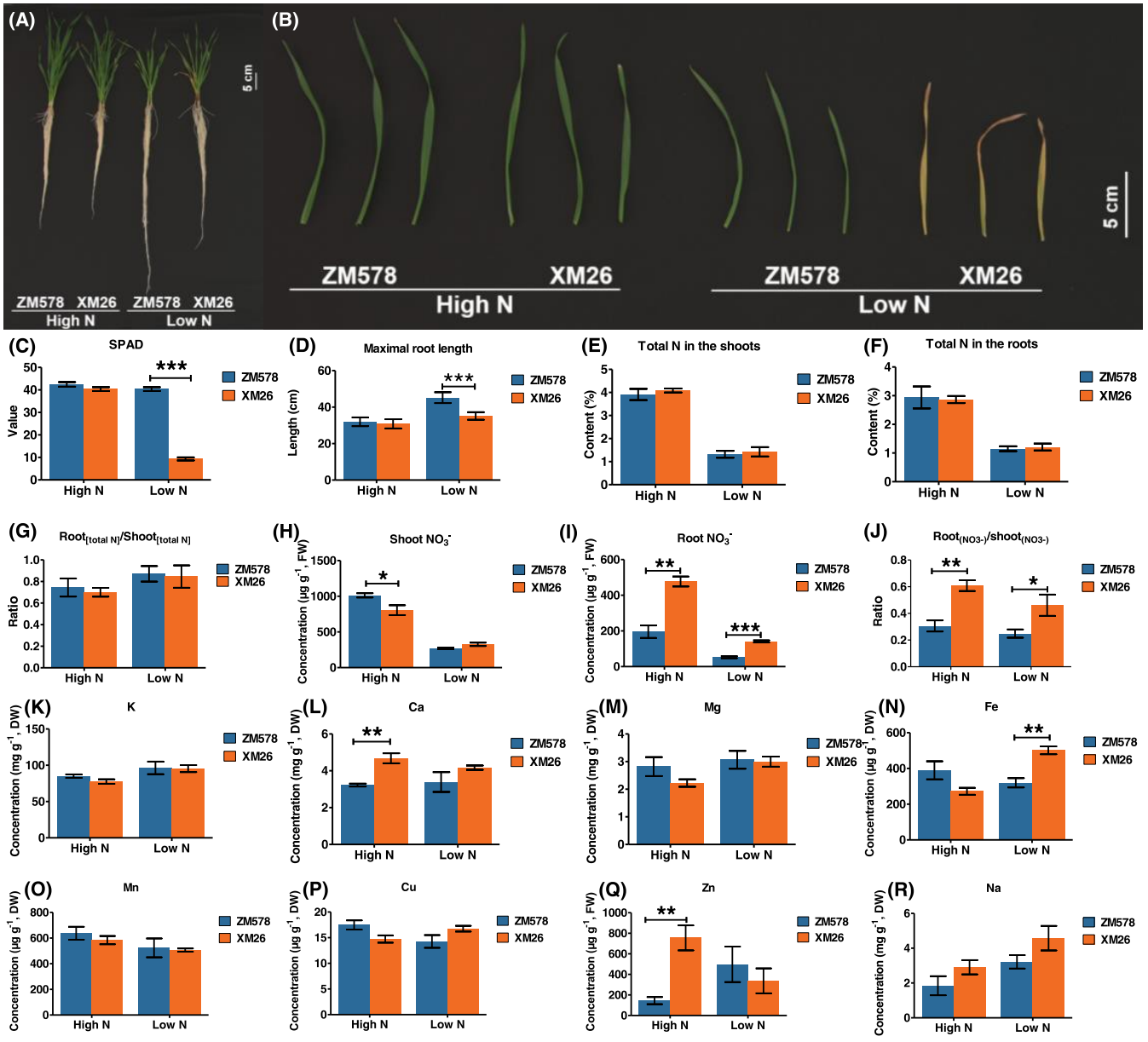

Figure 5. Differential morpho-physiological responses to nitrogen (N) deficiency between the low-N-tolerant and low-N-sensitive wheat genotypes. (A, B) Growth performance overview of the whole plants (A) and old leaves (B) of the low-N-tolerant cultivar Zhongmai 578 (ZM578) and the low-N-sensitive wheat cultivar Xinmai 26 (XM26) under high N and low N conditions. (C−R) Leaf SPAD values (C), maximal root length (D), total N in the shoots (E), total N in the roots (F), ratios of $root_{[total\ N]}/shoot_{[total\ N]}$ (G), total NO_3^- in the shoots (H), total NO_3^- in the roots (I), ratios of $root_{[NO_3^-]}/shoot_{[NO_3^-]}$ (J), and the concentrations of K (K), Ca (L), Mg (M), Fe (N), Mn (O), Cu (P), Zn (Q), and Na (R) in the old leaves of the low-N-tolerant cultivar ZM578 and the low-N-sensitive wheat cultivar XM26 under high N and low N conditions. Uniform wheat seedlings were hydroponically grown under high N (6.0 mM NO_3^-) and low N (0.30 mM NO_3^-) conditions for 20 days until sampling. Data are presented as mean (n = 5) ± s.d. Significant differences (*p < 0.05; **p < 0.01; ***p < 0.001) were determined by unpaired two-tailed Student's t tests between two groups using the SPSS 17.0 toolkit.

a total of 4013 and 3288 DEGs were uniquely identified in the shoots and roots, respectively, with 557 DEGs commonly found in the two organs (Figure 7B). The PCA result showed that different N levels, wheat genotypes, and organs exhibited significantly different transcriptomic features (Figure 6B). It was noteworthy that the GO terms of transporter activity, membrane, and response to stimuli were highly enriched in both shoots and roots under low N (Figure 6C). A KEGG analysis of the genome-wide DEGs showed that in addition to nitrate transport commonly identified in both shoots and roots (Figure 6D,E), the transport and metabolism of organic N nutrients (such as amine and amino acid) was characterized in the roots of wheat plants under low N (Figure 6F).

First, we investigated the concentration profiles of some phytohormones, namely, IAA, GA, ABA, JA, SA, BR, *t*Z, *c*Z, *t*ZR, 2-iPA, and BR, and their expression profiles in the shoots and roots between the low-N-tolerant cultivar ZM578 and the low-N-sensitive cultivar XM26 (Figure 7). Among these phytohormones, ABA, JA, and SA were the most noteworthy. The shoot ABA and root JA and SA presented significantly higher concentrations in XM26 than in ZM578 (Figure 7A). Based on the genes involved in the biosynthesis of these three

https://doi.org/10.1021/acs.jafc.3c08626
J. Agric. Food Chem. 2024, 72, 3814−3831

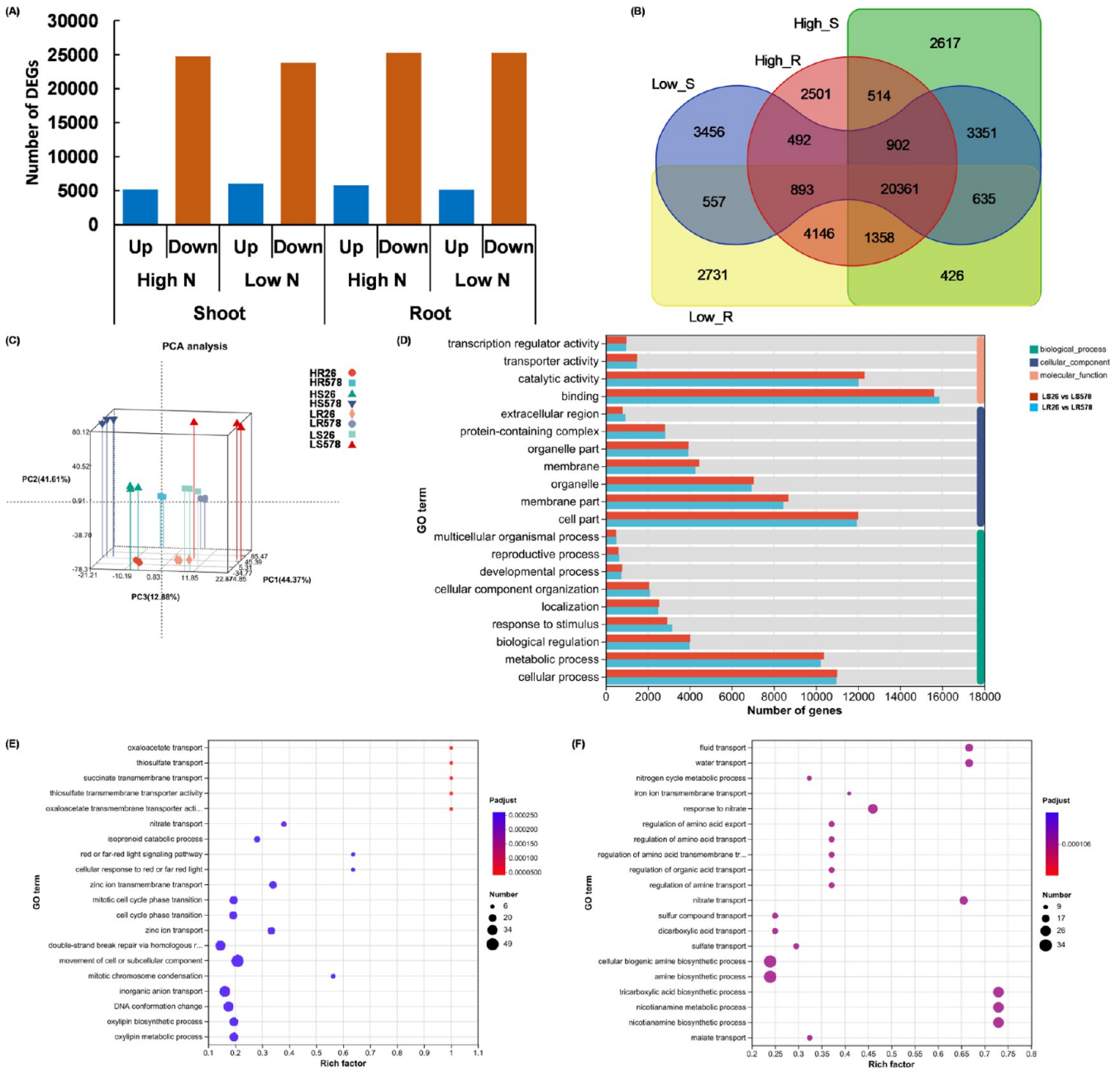

Figure 6. Overview of comparative transcriptome sequencing data from the low-nitrogen (N)-tolerant and low-N-sensitive wheat seedlings grown under high N and low N conditions. (A–F) Number (A), Venn diagram-mediated intersection analysis (B), principal component analysis (C), GO enrichment analysis (D), and KEGG pathway enrichment analysis in the shoots (E) and roots (F) of genome-wide differentially expressed genes (DEGs) of wheat plants grown under high N and low N conditions. H, high N; L, low N; S, shoot; R, root. Solid circle sizes represent the pathway enriched degree. The bigger the circles are, the more the corresponding KEGG items are. Regarding the RNA-seq experiment, the wheat plants that were grown under high N (6.0 mM NO_3^-) and low N (0.30 mM NO_3^-) for 20 days until the shoots and roots were individually sampled. False discovery rate (FDR) $\leq$ 0.05 and $\log_2$ (fold-change) $\geq$ 1.0 are used as the thresholds to identify DEGs.

phytohormones (Figure 7B), we found that the expression levels of *TaPBSs* and *TaEPSs* involved in SA biosynthesis, *TaLOXs* involved in JA biosynthesis, and *TaADHs* involved in the ABA biosynthesis showed higher expression levels in XM26 than in ZM578 (Figure 7C–E).

Considering that differential root-to-shoot NO_3^- translocation is the major reason for differential low N tolerance between the wheat genotypes (Figure 5J), *NPF7.3/NRT1.5*, responsible for root xylem NO_3^- loading, was proposed to be the candidate gene responsible for differential low N tolerance. Based on the comparative transcriptome sequencing data, we identified two *NPF7.3/NRT1.5* DEGs, among which is *TaNPF7.3/TaNRT1.5-6D* (Latest ID: TraesCS6D03G0593500; raw ID: TraesCS6D02G251500) was strongly induced by low N, and presented significantly higher expression levels in the roots of ZM578 than in the roots of XM26 (Figure 8A).

CLCa and CLCb are important transporters responsible for vacuolar NO_3^- influx and efflux.[35,36] Under low N, reduced *CLCa* expression and increased *CLCb* expression contributed to efficient long-distance NO_3^- translocation from roots to shoots, which was undertaken by the elevated expression of *NPF7.3/*

https://doi.org/10.1021/acs.jafc.3c08626
J. Agric. Food Chem. 2024, 72, 3814–3831

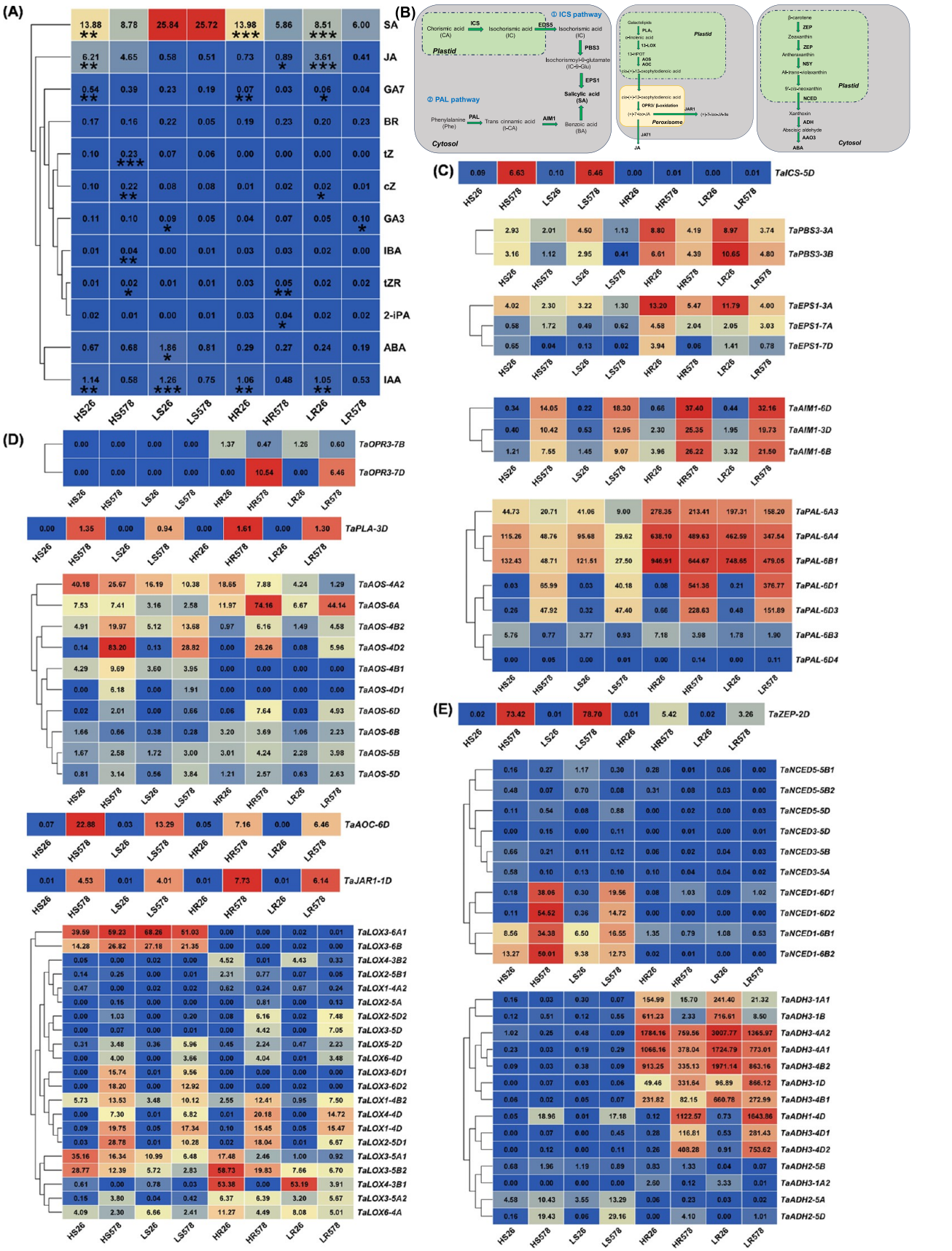

Figure 7. Phytohormone concentration profiles and transcriptional profiling of the genes involving the phytohormone biosynthesis in the shoots and roots of the low-nitrogen (N)-tolerant genotype ZM578 and the low-N-sensitive genotype XM26 grown under high N and low N conditions. (A) Phytohormone concentration profiles, (B−E) biosynthesis pathways (B) transcriptional profiling of the genome-wide genes involving the biosynthesis of ABA (C), JA (D), and SA (E) in the shoots and roots of ZM578 and XM26. H, (high N); L, low N; S, shoot; R, root. ABA, abscisic acid; BR,

https://doi.org/10.1021/acs.jafc.3c08626
J. Agric. Food Chem. 2024, 72, 3814−3831

Figure 7. continued

brassinosteroids; *cZ*, *cis*-Zeatin; GA, gibberellic acid; IAA, indole-3-acetic acid; IBA, indole-3-butyric acid; iP, isopentenyladenine; JA, jasmonic acid; SA, salicylic acid; *tZ*, *trans*-Zeatin; *tZR*, *trans*-zeatin riboside. AAO, abscisic aldehyde oxidase; ADH, alcohol dehydrogenase; AOC, allene oxide cyclase; AOS, allene oxide synthase; LOX, lipoxygenase; NCED, 9-cis-epoxycarotenoid dioxygenase; OPR, 12-oxo-phytodienoic acid reductase; PLA_1, phospholipase A_1; ZEP, zeaxanthin epoxidase; ZSY, neoxanthin synthase. Regarding the RNA-seq and phytohormone assay experiments, the wheat plants that were grown under high N (6.0 mM NO_3^-) and low N (0.30 mM NO_3^-) for 20 days until the shoots and roots were individually sampled. False discovery rate (FDR) $\leq$ 0.05 and $\log_2$ (fold-change) $\geq$ 1.0 are used as the thresholds to identify DEGs.

NRT1.5.[37] Therefore, we investigated the expression of *TaCLCa* and *TaCLCb* in the roots of ZM578 and XM26; we found that the low-N-tolerant cultivar ZM578 presented lower expression of *TaCLCa-6A* and higher expression of *TaCLCb-6D* than the low-N-sensitive cultivar XM26, particularly under N limitation (Figure 8B). We also found that the N-assimilation genes, particularly *TaNIA1−7D*/*TaNIA1−6D* and *TaGLN1;2−4D*/*TaGLN1;2−4D*, showed expression levels significantly higher in ZM578 than in XM26 (Figure 8C,D). The expression of organic N transporter genes (mainly *AAPs* and *UPSs*), particularly *TaAAP15-Un* and *TaUPS2−5D*, was significantly higher in ZM578 than in XM26 (Figure 8E,F). In addition, the higher expression of *ATGs* (particularly *TaATG8A-2D*) and *TaNLAs* (particularly *TaBAH-2D*) in ZM578 than in XM26 (Figure 8G,H) might indicate that ZM578 has a stronger tolerance against N limitation and more efficient N recycling.

Molecular Characterization of Candidate Gene *TaNPF7.3*/*TaNRT1.5−6D*, Responsible for Differential Low N Tolerance in Wheat Genotypes. In this study, *NPF7.3*/*NRT1.5* had three homologues in the genome of allohexaploid wheat, with one homologue in the A, B, and D subgenomes. We performed a comprehensive analysis of its molecular characteristics to better understand the key role of the aforementioned *TaNPF7.3*/*TaNRT1.5−6D*-mediated efficient root xylem NO_3^- loading in regulating differential low N tolerance between wheat genotypes. Gene structure analysis showed that the full-length genome of *TaNPF7.3*/*TaNRT1.5−6D* was 3554 bp, with three exons and two introns (Figure 9A). Through the isolation of full-length CDSs, we found that the sequences of both *TaNPF7.3*/*TaNRT1.5−6D*^{ZM578} and *TaNPF7.3*/*TaNRT1.5−6D*^{XM26} were identical to that in Chinese Spring. *TaNPF7.3*/*TaNRT1.5−6D* encoded 616 amino acids, and the molecular weight and pI of its protein were predicted to be 66.91 kDa and 6.5, respectively. Conserved domain analysis showed that *TaNPF7.3*/*TaNRT1.5−6D* belongs to a member of the major facilitator superfamily. *TaNPF7.3*/*TaNRT1.5−6D* was predicted to possess strong hydrophilicity (excluding the N- and C-terminus) with nine transmembrane domains (Figure 9B,C).

Expression pattern analysis showed that *TaNPF7.3*/*TaNRT1.5−6D* was mainly expressed in the roots from the seedling to tillering stages. From the flag leaf to milk grain stages, *TaNPF7.3*/*TaNRT1.5−6D* presented higher expression levels in the flag leaf sheath and shoot axis than in the other organs. At the dough stage, the expression of *TaNPF7.3*/*TaNRT1.5−6D* reached a peak in the hard dough (Figure 9D). Strong localization signals of *TaNPF7.3*/*TaNRT1.5−6D* consistent with FM4−64 indicated that *TaNPF7.3*/*TaNRT1.5−6D* functioned as a plasma-membrane-localized transporter (Figure 9E). Regulatory network analysis showed that the transcription factors of ERFs, NACs, MYBs, TALEs, bZIPs, and MADSs might be involved in the transcriptional regulation of *TaNPF7.3*/*TaNRT1.5−6D* (Figure 9F). To examine the transcriptional response of *TaNPF7.3*/*TaNRT1.5−6D* to other nutrient stresses (including low K, low Fe, salt stress, and saline-alkaline stress), we used RT-qPCR assays to test its expression levels. The expression of *TaNPF7.3*/*TaNRT1.5−6D* was strongly induced by K limitation (Figure 10A), salinity (Figure 10C), and saline-alkaline stress (Figure 10D), while it was not transcriptionally responsive to low Fe (Figure 10B).

Previous studies have reported that *Arabidopsis* ETHYLENE INSENSITIVE3 (EIN3), an ethylene response factor (ERF), binds to the EIN3-binding site motifs in the *NPF7.3*/*NRT1.5* promoter and represses its expression[38] (Figure 10E). The transcription factor MYB59 positively regulates the transcription of *Arabidopsis NPF7.3*/*NRT1.5* in response to low K stress[39] (Figure 10F). To determine whether the TaERF and TaMYB59 transcription factors were involved in the transcriptional regulation of *TaNPF7.3*/*TaNRT1.5*, we investigated and compared their expression profiles between the low-N-tolerant genotype ZM578 and the low-N-sensitive genotype XM26. *TaEIN 3s*/*TaEILs* presented significantly higher expression levels in the low-N-tolerant cultivar ZM578 (particularly roots), with higher *TaNPF7.3*/*TaNRT1.5−6D* expression, than in the low-N-sensitive cultivar XM26 (Figure 10G). However, among the three *TaMYB59* homologues, only *TaMYB59−3D* (TraesCS3D02G540600) showed differential expression between ZM578 and XM26, and it presented higher expression in ZM578 than in XM26 (Figure 10H). Moreover, we found that *TaMYB59−3D* was mainly expressed in the roots, showing a similar expression preference to *TaNPF7.3*/*TaNRT1.5−6D* (Figure 10I). Taken together, we propose that *TaMYB59−3D* might function as a key transcription factor positively regulating the expression of *TaNPF7.3*/*TaNRT1.5−6D*, which confers more efficient root-to-shoot NO_3^- translocation and leaf-to-sinks interaction in the low-N-tolerant cultivar ZM578.

DISCUSSION

In terms of the molecular mechanisms underlying efficient N use in the three major cereal crop species, namely, rice, maize, and wheat, although great progress has been made in rice[40,41] and maize,[42,43] few noticeable achievements have been obtained in wheat.[35] Plants tend to retain N in source organs when N nutrients are sufficient; when the N status is relatively low, plants remobilize N more efficiently.[44] Therefore, NUE is usually significantly higher under low N conditions than under high N conditions.[45] In this study, hydroponic culture, ICP-MS, NMT, HPLC, RNA-seq, and bioinformatics were integrated to identify the growth performance of wheat plants grown under high N and low N conditions, ion and phytohormone profiles, and genome-wide differential expression profiling and further uncover the regulatory mechanism underlying NUE and low N tolerance. The transcriptional profiling of *NPFs*, *NRT2s*, *CLCs*, *SLACs*/*SLAHs*, *AAPs*, and *UPSs* characterized the core members involved in the efficient transport of nitrate and organic N nutrients. In a word, relative to XM26, a stronger low N tolerance in ZM578 might be related to efficient root-to-shoot nitrate translocation, source leaves to sinks remobilization of

https://doi.org/10.1021/acs.jafc.3c08626
J. Agric. Food Chem. 2024, 72, 3814−3831

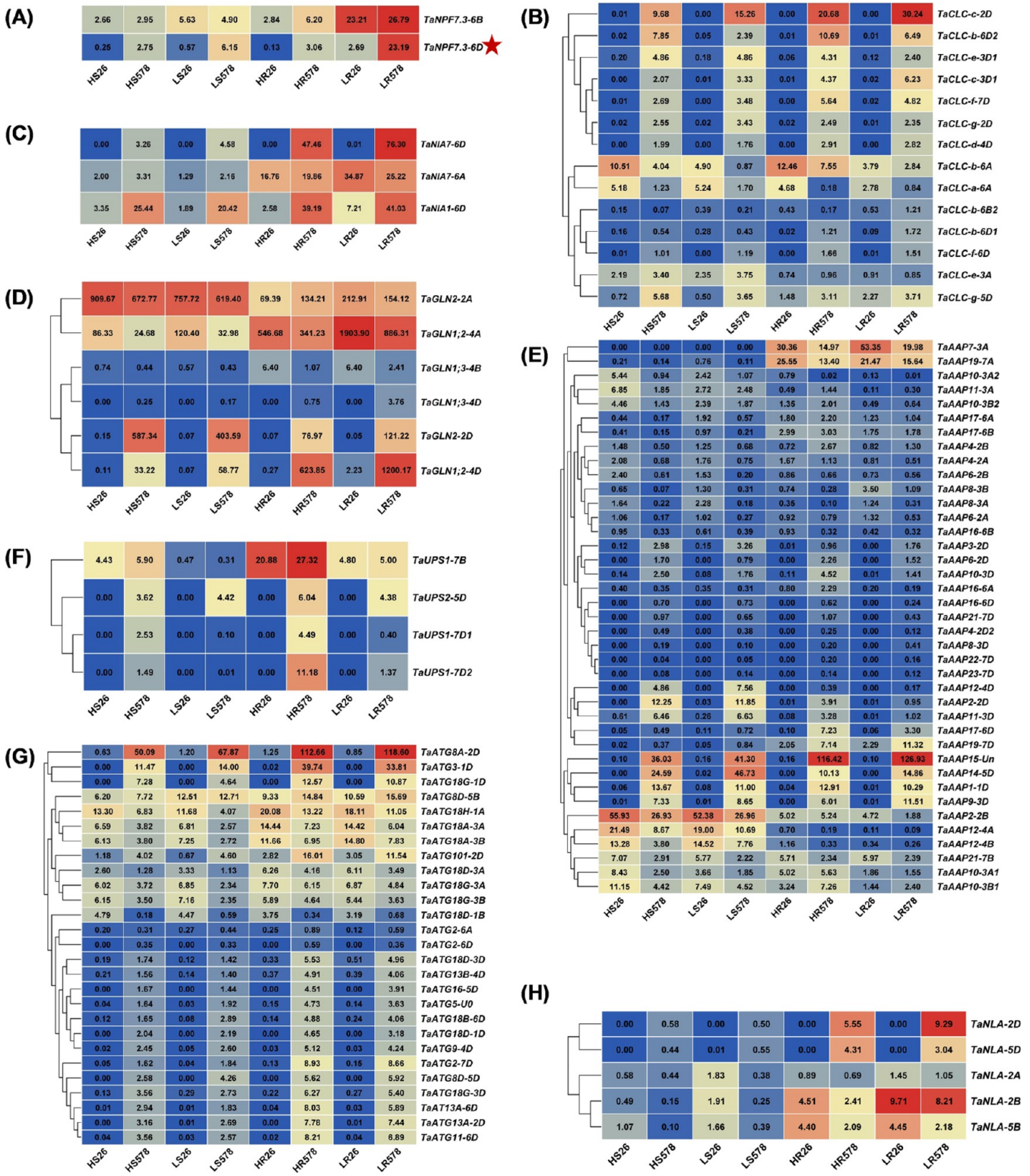

Figure 8. Transcriptional identification of the core transporter and key nitrogen (N) metabolism-related genes in the shoots and roots of the low-N-tolerant and -sensitive wheat plants grown under high N and low N conditions. (A–H) Differential expression profiling of the (A) NPF7.3/NRT1.5, (B) CLC, (C) nitrate reductase (NIA), (D) glutamine synthetase (GLN), (E) amino acid permease (AAP), (F) ureide permease (UPS), (G) autophagy-related gene (ATG), and (H) nitrogen limitation adaptation (NLA) genes in the shoots and roots of wheat plants grown under high N and low N conditions. Regarding the RNA-seq experiment, the wheat plants that were grown under high N (6.0 mM NO_3^-) and low N (0.30 mM NO_3^-) for 20 days until the shoots and roots were individually sampled. False discovery rate (FDR) $\leq$ 0.05 and $\log_2$ (fold-change) $\geq$ 1.0 are used as the thresholds to identify DEGs. H, (high N); L, low N; S, shoot; R, root.

nitrate, vacuolar nitrate release, organic N remobilization, and N assimilation (Figure 11). The *TaMYB59–3D-TaNPF7.3/NRT1.5–6D* module was proposed as an important pathway regulating differential responses of wheat genotypes to low N.

https://doi.org/10.1021/acs.jafc.3c08626
J. Agric. Food Chem. 2024, 72, 3814–3831

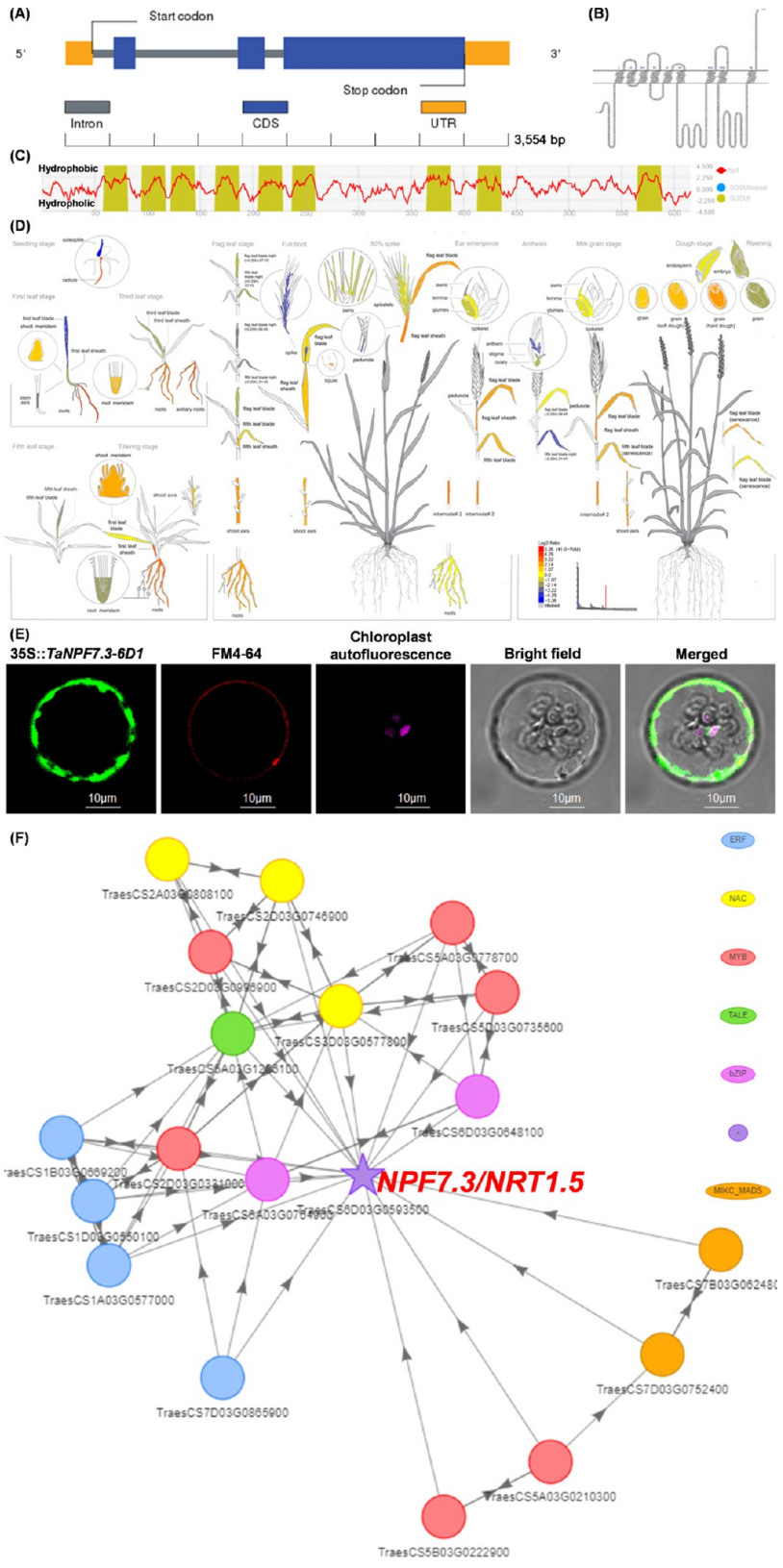

Figure 9. Molecular characterization of *TaNPF7.3/TaNRT1.5−6D* (Latest ID: TraesCS6D03G0593500; raw ID: TraesCS6D02G251500) in allohexaploid wheat. (A−C) Gene structure (A), secondary structure (B), and hydrophobicity plot (C) of *TaNPF7.3/TaNRT1.5−6D*. Hydrophobicity and hydrophilicity of the amino acids were defined by positive and negative values. (D−F) Tissue-specific expression patterns of *TaNPF7.3/TaNRT1.5−6D* in wheat plants at the whole growth stages. The expression profiling was retrieved from the wheat eFP browser (https://bar.utoronto.ca/efp_wheat/cgibin/efpWeb.cgi). The darker the color of heat maps, the higher the gene expression levels. (F) Analysis of transcriptional regulatory network involving *TaNPF7.3/TaNRT1.5−6D* in the wGRN database (http://wheat.cau.edu.cn/wGRN/). Different colored boxes indicate different transcription factors.

https://doi.org/10.1021/acs.jafc.3c08626
J. Agric. Food Chem. 2024, 72, 3814−3831

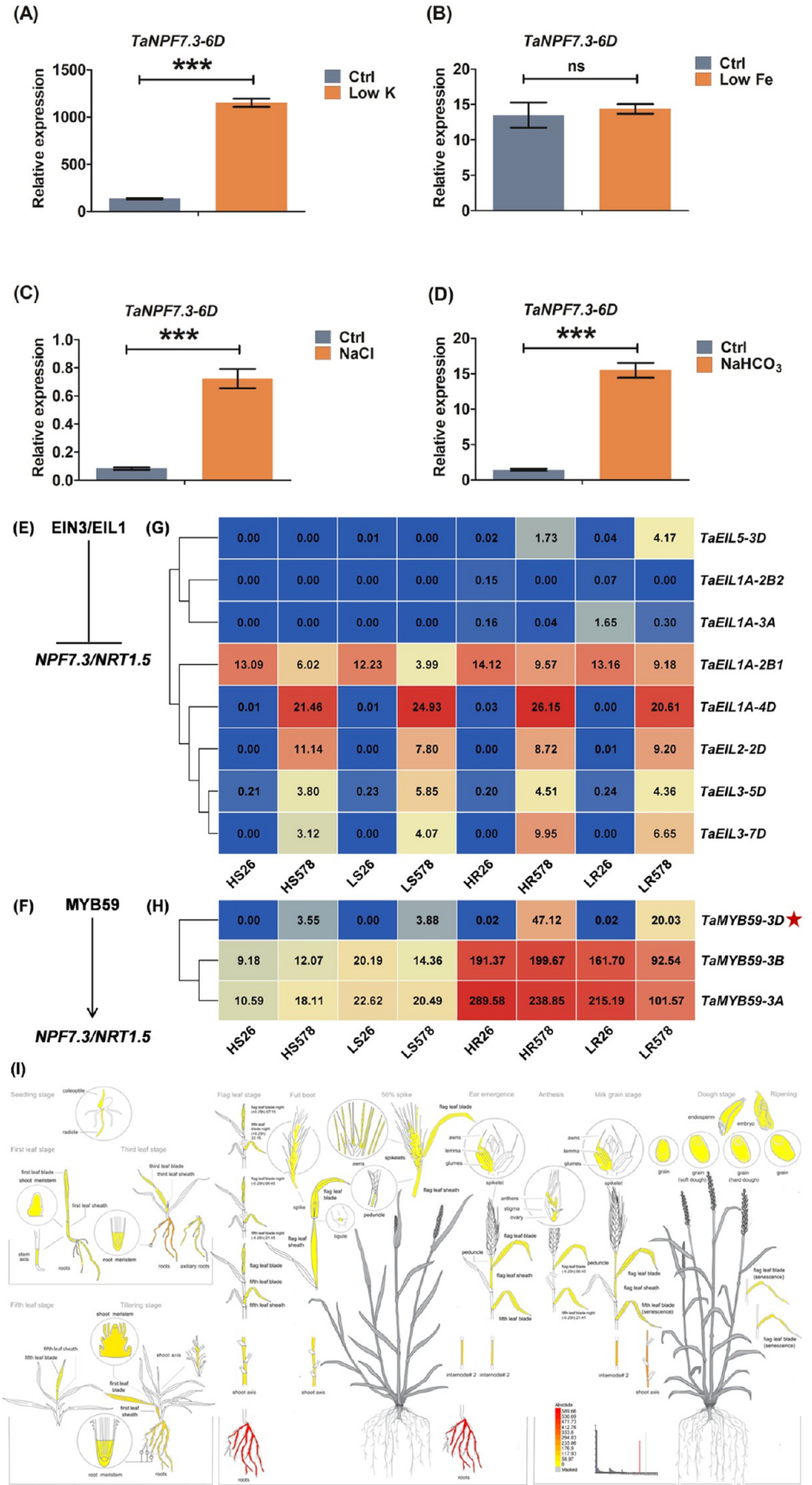

Figure 10. Transcriptional responses of *TaNPF7.3/TaNRT1.5−6D* to multiple nutrient stresses and identification of potential transcription factors regulating the expression of *TaNPF7.3/TaNRT1.5−6D*. (A−D) Relative expression of *TaNPF7.3/TaNRT1.5−6D* under low K (A), low Fe (B), salt stress (C), and saline-alkaline stress (D). Ctrl, control. Regarding the low-K treatment, the wheat plants that were grown under high K/control (6.0 mM) and low N (0.03 mM NO_3^-) for 20 days until the roots were sampled. Regarding the low-Fe treatment, the wheat plants that were grown under

https://doi.org/10.1021/acs.jafc.3c08626
J. Agric. Food Chem. 2024, 72, 3814−3831

Figure 10. continued

high Fe/control (50 μM EDTA-Fe) and low Fe (2.0 μM EDTA-Fe) for 20 days until the roots were sampled. Regarding the salt stress treatment, the wheat plants that were grown under control (salt-free) and salt stress (100 mM NaCl) for 20 days until the roots were sampled. Regarding the saline-alkaline stress treatment, the wheat plants that were grown under control (salt-free) and saline-alkaline (75 mM $NaHCO_3$) for 20 days until the roots were sampled. Data are presented as mean (n = 3) ± s.d. Significant differences were determined using Student's t test: ns, not significant; *P < 0.05; **P < 0.01; ***P < 0.001. (E, F) Reported EIN3/EIL-mediated negative and MYB59-mediated positive transcriptional regulation of the *TaNPF7.3/TaNRT1.5–6D* expression (Zhang et al., 2014; Du et al., 2019). (G, H) Transcriptional profiling of the transcription factor gens *EIN3/EIL* and *MYB59* in the shoots and roots of the low-nitrogen (N)-tolerant genotype ZM578 and the low-N-sensitive genotype XM26 grown under high N and low N conditions. Regarding the RNA-seq and phytohormone assay experiments, the wheat plants that were grown under high N (6.0 mM NO_3^-) and low N (0.30 mM NO_3^-) for 20 days until the shoots and roots were individually sampled. False discovery rate (FDR) ≤ 0.05 and $\log_2$ (fold-change) ≥ 1.0 are used as the thresholds to identify DEGs. (I) Tissue-specific expression patterns of *TaMYB59-D* (TraesCS3D02G540600) in wheat plants at the whole growth stages. The expression profiling was retrieved from the wheat eFP browser (https://bar.utoronto.ca/efp_wheat/cgibin/efpWeb.cgi). The darker the color of heat maps, the higher the gene expression levels.

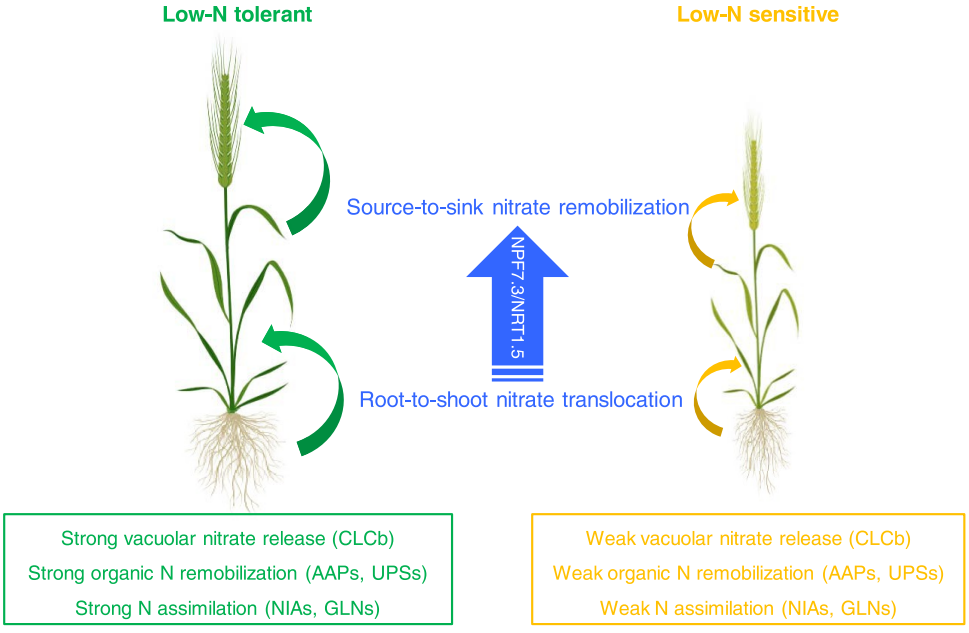

Figure 11. Model showing molecular mechanisms underlying differential low N tolerance between wheat genotypes. The arrow sizes indicate the degrees of N transport with wheat plants.

These findings provide some elite candidate genes for the selection and breeding of wheat germplasm with a low N tolerance and high NUE.

Great Divergence in Expression Preference within One Family or Among Plant Species. Duplicated genes widely occurring in alloploidy crop species provide novel resources for the formation of new genes, which, in turn, contribute to gene loss, neo-functionalization, and subfunctionalization.[46] In this study, we found that in allohexaploid wheat multicopy gene formation was ubiquitous in numerous N transporter families. The gene-specific expression tissues, expression abundances, and N-responsive patterns, among others, were significantly distinct among the gene family members (Figures 3, 4, 7, and 8). Based on the expression profiling, we easily distinguished the core members playing important roles in the regulation of low-N responses and NUE. For example, *TaNPF6.3–1D1* (raw ID: TraesCS1D02G214200; latest ID: TraesCS1D03G0536100) showed the highest expression abundance, which was significantly higher than that of the other *NPF* family members (Figure 3A). This result might be used as a good reference for the selection of candidate genes when performing the genetic modification of low N tolerance and NUE in wheat. Moreover, we also found that great divergence in the gene expression of N transporters occurred between monocots and dicots. For example, in *Arabidopsis thaliana* and rapeseed (*Brassica napus* L.), *AtNRT2.1* and *BnaNRT2.1s* presented the highest transcript levels.[29,47] However, besides *OsNRT2.1*, *OsNRT2.4* showed a very high expression level relative to other *NRT2* members in rice.[48] In rapeseed, *BnaNRT2.3s* showed very low expression abundances within the *BnaNRT2.1* family,[29] while *TaNRT2.3s* presented very high expression levels within the *TaNRT2* family (Figure 3B).

Among the divergent nitrate transporters between monocots and dicots, we paid great attention to AtNRT1.7/AtNPF2.13, which is expressed mainly in the phloem of leaf minor veins and mediates the remobilization of excess NO_3^- from older leaves to younger ones.[4] In *Arabidopsis*, NLA acting as an E3 ubiquitin ligase mediates the degradation of NPF2.13/NRT1.7, and contributes to the efficient remobilization of N from source leaves to sink organs; moreover, the expression of AtNLA1 is not transcriptionally regulated by N levels.[49] Enhancing source-to-sink NO_3^- remobilization by overexpressing *NPF2.13/NRT1.7* has been shown to be a key strategy for enhancing NUE and crop production.[50] However, we could not detect the expression of *NPF2.13/NRT1.7* in either the shoots or roots of the three wheat cultivars (Chinese Spring, ZM578, and XM26) grown under high and low N conditions. Moreover, the function of

https://doi.org/10.1021/acs.jafc.3c08626
J. Agric. Food Chem. 2024, 72, 3814–3831

NPF2.13/NRT1.7 has not yet been reported in rice. Therefore, we presumed that source-to-sink NO_3^- remobilization might be undertaken by other transporters, not *NPF2.13/NRT1.7* in wheat. In this study, some *NLA* homologues in wheat were transcriptionally responsive to low N (Figures 4G and 7H), indicating their distinct expression patterns in wheat from those of *NLA* in *Arabidopsis*.[49]

Multifaceted Roles of *NPF7.3/NRT1.5* in Regulating the Growth, Development, and Responses of Plants to Stress. *AtNPF7.3/AtNRT1.5*, driving root-to-shoot NO_3^- translocation,[51] is also involved in modulating the response to K^+ deprivation in *Arabidopsis*.[52] Functional disruption of *NPF7.3/NRT1.5* enhanced tolerance to salt stress, drought, and cadmium toxicity.[53] *NPF7.3/NRT1.5* functions as a transporter of indole-3-butyric acid (IBA), a precursor of the major endogenous auxin indole-3-acetic acid (IAA).[46,54] In this study, *TaNPF7.3/TaNRT1.5−6D* was mainly expressed in the roots of wheat plants at the vegetative stage, and *TaNPF7.3/TaNRT1.5−6D* showed a dominant expression preference in the flag leaves and grains at the reproductive stage (Figure 9D) when the abilities of senescent wheat roots to absorb N were greatly decreased. The expression pattern of *TaNPF7.3/TaNRT1.5−6D* combined with the function of *Arabidopsis NPF7.3/NRT1.5* suggested that *TaNPF7.3/TaNRT1.5−6D* might be involved in root-to-shoot NO_3^- translocation and remobilization of NO_3^- from source organs to sinks (Figure 11). Considering that *NPF7.3/NRT1.5* is involved in the regulation of K starvation-induced leaf senescence,[52] we made a comparison of the K^+ concentrations in the senescent leaves under low N. However, there were no obvious differences in the leaf K^+ concentrations between the low-N-tolerant genotype ZM578 and the low-N-sensitive genotype XM26 (Figure 5K). Therefore, we propose that K^+ is not involved in the differential responses of ZM578 and XM26 to low N. Previous studies have reported that ethylene and JA signaling mediates the downregulation of *NPF7.3/NRT1.5* via ethylene response factors (ERFs), including EIN3/EIL1, which further modulate stress tolerance and plant growth.[38] MYB59 responds to low K^+ stress and directs root-to-shoot K^+/NO_3^- translocation by regulating the expression of *NPF7.3/NRT1.5* in *Arabidopsis* roots.[39] In this study, based on the differential expression profile of *TaEIN 3s/EILs* and *TaMYB59s* between the low-N-tolerant and low-N-sensitive cultivars (Figure 10G,H), we propose that TaMYB59−3D might be involved in the positive transcriptional regulation of *TaNPF7.3/NRT1.5−6D*. Taken together, the TaMYB59−3D-*TaNPF7.3/TaNRT1.5−6D* module might play a pivotal role in efficient long-distance root-to-shoot NO_3^- translocation and source leaf-to-sink NO_3^- remobilization, which further contributed to the improvement of low N tolerance and NUE.

■ ASSOCIATED CONTENT

Data Availability Statement

All of the data and materials that are required to reproduce these findings can be shared by contacting the corresponding author, Dr. Ying-peng Hua (yingpenghua@zzu.edu.cn).

Supporting Information

The Supporting Information is available free of charge at https://pubs.acs.org/doi/10.1021/acs.jafc.3c08626.

Consistency analysis between the RT-qPCR assays and RNA-seq results (Figure S1); overview of transcriptome sequencing data from wheat seedlings grown under high N and low N conditions (Figure S2); gene ontology (GO) analysis of genome-wide differentially expressed genes in the shoots (A) and roots (B) of wheat plants (cv. Chinese Spring) grown under high N and low N conditions (Figure S3); Kyoto Encyclopedia of Genes and Genomes (KEGG) enrichment analysis of genome-wide differentially expressed genes in the shoots (A) and roots (B) of wheat plants (cv. Chinese Spring) grown under high N and low N conditions (Figure S4); overview of the transcriptome sequencing data of wheat plants (cv. Chinese Spring) grown under high N and low N conditions (Table S1); and overview of the transcriptome sequencing data between the low-N-tolerant and low-N-sensitive wheat genotypes (Table S3) (PDF)

List of gene IDs and gene names (Table S2) (XLSX)

■ AUTHOR INFORMATION

Corresponding Authors

Peng-jia Wu − *School of Agricultural Sciences, Zhengzhou University, Zhengzhou 450001, China*; Email: wupengjia0905@163.com

Ying-peng Hua − *School of Agricultural Sciences, Zhengzhou University, Zhengzhou 450001, China*; orcid.org/0000-0002-5730-3737; Phone: +86-15084873150; Email: yingpenghua@zzu.edu.cn; Fax: 0371-67785095

Authors

Qiong Li − *Department of Brewing Engineering, Moutai Institute, Renhuai 564507 Guizhou, China*

Hai-li Song − *School of Agricultural Sciences, Zhengzhou University, Zhengzhou 450001, China*

Ting Zhou − *School of Agricultural Sciences, Zhengzhou University, Zhengzhou 450001, China*

Min-nan Pei − *School of Agricultural Sciences, Zhengzhou University, Zhengzhou 450001, China*

Bing Wang − *Department of Brewing Engineering, Moutai Institute, Renhuai 564507 Guizhou, China*

Song-xian Yan − *Department of Resources and Environment, Moutai Institute, Renhuai 564507 Guizhou, China*

Yun-qi Liu − *Zhongguancun Xuyue Non-invasive Micro-test Technology Industrial Alliance, Beijing 10080, China*

Complete contact information is available at: https://pubs.acs.org/10.1021/acs.jafc.3c08626

Author Contributions

Y.P.H. and T.Z. conceptualized the project and were responsible for acquiring the funding; Y.P.H., T.Z., Q.L., P.J.W., B.W., and S.X.Y. performed the experiments; Y.P.H., P.J.W., Y.Q.L., and T.Z. analyzed and interpreted the data; Y.P.H. wrote the paper with significant input from all of the other authors. All authors reviewed the manuscript.

Funding

This study was financially supported by the key area projects of Guizhou education department (KY[2020]044) and the Ministry of Education's new agricultural research and reform practice project ([2020]80), China Postdoctoral Science Foundation (2022M722876), and National Key R&D Program of China (2021YFD1700900).

Notes

The authors declare no competing financial interest.

■ ACKNOWLEDGMENTS

The authors are very grateful to the editor and reviewers for critically evaluating the manuscript and providing constructive comments for its improvement. Thanks go to Longfei Zheng [Bapu (Shanghai) Information Sci. & Tech. Co., Ltd.] for the technical support in the noninvasive microtest technology (NMT) experiment. The authors also thank LetPub (www.letpub.com) for its linguistic assistance during the preparation of this manuscript.

■ ABBREVIATIONS

AAP:amino acid permease; AAT:amino acid transporter; DEGs:differentially expressed genes; N:nitrogen; NCBI:National Center for Biotechnology Information; NH_4^+:ammonium; NO_3^-:nitrate; NUE:nitrogen use efficiency; TF:transcription factor; GS:glutamine synthetase; GOGAT:-glutamine synthase; NIA:nitrate reductase; NLA:nitrogen limitation adaptation; NPF:nitrate/peptide family; NR:nitrate reductase; NRT:nitrate transporter; MYB:v-myb avian myeloblastosis viral oncogene homologue; CLC:chloride channel; SLAC/SLAH:slowly activating anion channel; LATS:low-affinity transporter systems; HATS:high-affinity transporter systems; UPS:ureide permease; ABA:abscisic acid; BR:brassinosteroids; *cZ*:*cis*-Zeatin; GA:gibberellic acid; IAA:indole-3-acetic acid; IBA:indole-3-butyric acid; iP:isopentenyladenine; JA:jasmonic acid; SA:salicylic acid; *tZ*:*trans*-Zeatin; *tZR*:*trans*-zeatin riboside; AAO:abscisic aldehyde oxidase; ADH:alcohol dehydrogenase; AOC:allene oxide cyclase; AOS:allene oxide synthase; LOX:lipoxygenase; NCED:9-*cis*-epoxycarotenoid dioxygenase; OPR:12-oxo-phytodienoic acid reductase; PLA_1:phospholipase A_1; ZEP:zeaxanthin epoxidase; ZSY:neoxanthin synthase

■ REFERENCES

(1) Wang, Y. Y.; Cheng, Y. H.; Chen, K. E.; Tsay, Y. F. Nitrate transport, signaling, and use efficiency. *Annu. Rev. Plant Biol.* **2018**, *69*, 85−122.
(2) Xu, G.; Fan, X.; Miller, A. J. Plant nitrogen assimilation and use efficiency. *Annu. Rev. Plant Biol.* **2012**, *63*, 153−182.
(3) Xiao, J.; Liu, B.; Yao, Y.; et al. Wheat genomic study for genetic improvement of traits in China. *Sci. China Life Sci.* **2022**, *65* (9), 1718−1775.
(4) Zörb, C.; Ludewig, U.; Hawkesford, M. J. Perspective on wheat yield and quality with reduced nitrogen supply. *Trends Plant Sci.* **2018**, *23* (11), 1029−1037.
(5) Cui, Z. L.; Zhang, H. Y.; Chen, X. P.; et al. Pursuing sustainable productivity with millions of smallholder farmers. *Nature* **2018**, *555* (7696), 363−366.
(6) Liu, L.; Sadras, V. O.; Xu, J.; Hu, C.; Yang, X.; Zhang, S. Genetic improvement of crop yield, grain protein and nitrogen use efficiency of wheat, rice and maize in China. *Adv. Agron.* **2021**, *168*, 203−252.
(7) International Wheat Genome Sequencing Consortium (IWGSC). A chromosome-based draft sequence of the hexaploid bread wheat (*Triticum aestivum*) genome. *Science* **2014**, *345* (6194), No. 1251788, DOI: 10.1126/science.1251788.
(8) Islam, S.; Zhang, J.; Zhao, Y.; She, M.; Ma, W. Genetic regulation of the traits contributing to wheat nitrogen use efficiency. *Plant Sci.* **2021**, *303*, No. 110759.
(9) Vidal, E. A.; Alvarez, J. M.; Araus, V.; Riveras, E.; Brooks, M. D.; Krouk, G.; Ruffel, S.; Lejay, L.; Crawford, N. M.; Coruzzi, G. M.; Gutiérrez, R. A. Nitrate in 2020: Thirty years from transport to signaling networks. *Plant Cell* **2020**, *32* (7), 2094−2119.
(10) Tegeder, M. Transporters involved in source to sink partitioning of amino acids and ureides: opportunities for crop improvement. *J. Exp. Bot.* **2014**, *65* (7), 1865−1878.
(11) Caputo, C.; Barneix, A. J. Export of amino acids to the phloem in relation to N supply in wheat. *Physiol. Plant.* **1997**, *101*, 853−860.
(12) Simpson, R. J.; Dalling, M. J. Nitrogen redistribution during grain growth in wheat (*Triticum aestivum* L.): III. Enzymology and transport of amino acids from senescing flag leaves. *Planta* **1981**, *151* (5), 447−456.
(13) Barneix, A. J. Physiology and biochemistry of source-regulated protein accumulation in the wheat grain. *J. Plant Physiol.* **2007**, *164* (5), 581−590.
(14) Tegeder, M.; Rentsch, D. Uptake and partitioning of amino acids and peptides. *Mol. Plant* **2010**, *3* (6), 997−1011.
(15) Hawkesford, M. J. Genetic variation in traits for nitrogen use efficiency in wheat. *J. Exp. Bot.* **2017**, *68* (10), 2627−2632.
(16) Wang, H.; McCaig, T. N.; DePauw, R. M.; Clarke, J. M. Flag leaf physiological traits in two high-yielding Canada Western Red Spring wheat cultivars. *Can. J. Plant Sci.* **2008**, *88*, 35−42.
(17) Hu, M. Y.; Zhao, X. Q.; Liu, Q.; Hong, X.; Zhang, W.; Zhang, Y. J.; Sun, L. J.; Li, H.; Tong, Y. P. Transgenic expression of plastidic glutamine synthetase increases nitrogen uptake and yield in wheat. *Plant Biotechnol. J.* **2018**, *16* (11), 1858−1867.
(18) Armijo, G.; Gutiérrez, R. A. Emerging players in the nitrate ssignaling pathway. *Mol. Plant* **2017**, *10* (8), 1019−1022.
(19) Yang, J. B.; Wang, M. Y.; Li, W. J.; He, X.; Teng, W.; Ma, W.; Zhao, X.; Hu, M. Y.; Li, H.; Zhang, Y. J.; Tong, Y. P. Reducing expression of a nitrate-responsive bZIP transcription factor increases grain yield and N use in wheat. *Plant Biotechnol. J.* **2019**, *17* (9), 1823−1833.
(20) Hua, Y. P.; Zhou, T.; Huang, J. Y.; Yue, C. P.; Song, H. X.; Guan, C. Y.; Zhang, Z. H. Genome-wide differential DNA methylation and miRNA expression profiling reveals epigenetic regulatory mechanisms underlying nitrogen-limitation-triggered adaptation and use efficiency enhancement in allotetraploid rapeseed. *Int. J. Mol. Sci.* **2020**, *21* (22), 8453.
(21) Hoagland, D. R.; Arnon, D. I. The water-culture method for growing plants without soil. *Circular Calif. Agri. Exp. Stat. Publ.* **1950**, *347*, 32 DOI: 10.5555/19500302257.
(22) Zhang, Z. H.; Zhou, T.; Tang, T. J.; Song, H. X.; Guan, C. Y.; Huang, J. Y.; Hua, Y. P. A multiomics approach reveals the pivotal role of subcellular reallocation in determining rapeseed tolerance to cadmium toxicity. *J. Exp. Bot.* **2019**, *70* (19), 5437−5455.
(23) Zhou, T.; Hua, Y. P.; Xu, F. S. Involvement of reactive oxygen species and Ca^{2+} in the differential responses to low-boron in rapeseed genotypes. *Plant Soil* **2017**, *419* (1−2), 219−236.
(24) Patterson, K.; Cakmak, T.; Cooper, A.; Lager, I. D.; Rasmusson, A. G.; Escobar, M. A. Distinct signalling pathways and transcriptome response signatures differentiate ammonium- and nitrate-supplied plants. *Plant, Cell Environ.* **2010**, *33* (9), 1486−1501, DOI: 10.1111/j.1365-3040.2010.02158.x.
(25) Dudziak, K.; Sozoniuk, M.; Szczerba, H.; Kuzdraliński, A.; Kowalczyk, K.; Börner, A.; Nowak, M. Identification of stable reference genes for qPCR studies in common wheat (*Triticum aestivum* L.) seedlings under short-term drought stress. *Plant Method* **2020**, *16*, 58.
(26) Livak, K. J.; Schmittgen, T. D. Analysis of relative gene expression data using real-time quantitative PCR and the 2(-Delta Delta C(T)) Method. *Methods* **2001**, *25* (4), 402−408.
(27) Forde, B. G. Nitrate transporters in plants: structure, function and regulation. *Biochim. Biophys. Acta, Biomembr.* **2000**, *1465* (1−2), 219−235, DOI: 10.1016/S0005-2736(00)00140-1.
(28) Buchner, P.; Hawkesford, M. J. Complex phylogeny and gene expression patterns of members of the NITRATE TRANSPORTER 1/PEPTIDE TRANSPORTER family (NPF) in wheat. *J. Exp. Bot.* **2014**, *65* (19), 5697−5710.
(29) Hua, Y. P.; Zhou, T.; Song, H. X.; Guan, C. Y.; Zhang, Z. H. Integrated genomic and transcriptomic insights into the two-component high-affinity nitrate transporters in allotetraploid rapeseed. *Plant Soil* **2018**, *427*, 245−268.
(30) Kumar, A.; Sandhu, N.; Kumar, P.; Pruthi, G.; Singh, J.; Kaur, S.; Chhuneja, P. Genome-wide identification and *in silico* analysis of NPF,

NRT2, CLC and SLAC1/SLAH nitrate transporters in hexaploid wheat (*Triticum aestivum*). *Sci. Rep.* **2022**, *12* (1), No. 11227.
(31) Liao, Q.; Zhou, T.; Yao, J. Y.; Han, Q. F.; Song, H. X.; Guan, C. Y.; Hua, Y. P.; Zhang, Z. H. Genome-scale characterization of the vacuole nitrate transporter *Chloride Channel (CLC)* genes and their transcriptional responses to diverse nutrient stresses in allotetraploid rapeseed. *PLoS One* **2018**, *13* (12), No. e0208648.
(32) Melino, V. J.; Tester, M. A.; Okamoto, M. Strategies for engineering improved nitrogen use efficiency in crop plants via redistribution and recycling of organic nitrogen. *Curr. Opin. Biotechnol.* **2022**, *73*, 263−269.
(33) Carter, A. M.; Tegeder, M. Increasing nitrogen fixation and seed development in soybean requires complex adjustments of nodule nitrogen metabolism and partitioning processes. *Curr. Biol.* **2016**, *26* (15), 2044−2051.
(34) Redillas, M. C. F. R.; Bang, S. W.; Lee, D. K.; Kim, Y. S.; Jung, H.; Chung, P. J.; Suh, J. W.; Kim, J. K. Allantoin accumulation through overexpression of ureide permease1 improves rice growth under limited nitrogen conditions. *Plant Biotechnol. J.* **2019**, *17* (7), 1289−1301.
(35) Hodin, J.; Lind, C.; Marmagne, A.; Espagne, C.; Bianchi, M. W.; De Angeli, A.; Abou-Choucha, F.; Bourge, M.; Chardon, F.; Thomine, S.; Filleur, S. Proton exchange by the vacuolar nitrate transporter CLCa is required for plant growth and nitrogen use efficiency. *Plant Cell* **2023**, *35* (1), 318−335.
(36) Shi, Y.; Liu, D.; He, Y.; Tang, J.; Chen, H.; Gong, P.; Luo, J. S.; Zhang, Z. CHLORIDE CHANNEL-b mediates vacuolar nitrate efflux to improve low nitrogen adaptation in Arabidopsis. *Plant Physiol.* **2023**, *193* (3), 1987−2002.
(37) Han, Y. L.; Song, H. X.; Liao, Q.; Yu, Y.; Jian, S. F.; Lepo, J. E.; Liu, Q.; Rong, X. M.; Tian, C.; Zeng, J.; Guan, C. Y.; Ismail, A. M.; Zhang, Z. H. Nitrogen use efficiency is mediated by vacuolar nitrate sequestration capacity in roots of *Brassica napus*. *Plant Physiol.* **2016**, *170* (3), 1684−1698.
(38) Zhang, G. B.; Yi, H. Y.; Gong, J. M. The Arabidopsis ethylene/jasmonic acid-NRT signaling module coordinates nitrate reallocation and the trade-off between growth and environmental adaptation. *Plant Cell* **2014**, *26* (10), 3984−3998.
(39) Du, X. Q.; Wang, F. L.; Li, H.; Si, J.; Yu, M.; Li, J.; Wu, W.; Kudla, J.; Wang, Y. The transcription factor MYB59 regulates K^+/NO_3^- translocation in the Arabidopsis response to low K^+ stress. *Plant Cell* **2019**, *31* (3), 699−714.
(40) Li, S.; Tian, Y.; Wu, K.; Ye, Y.; Yu, J.; Zhang, J.; Liu, Q.; Hu, M.; Li, H.; Tong, Y.; Harberd, N. P.; Fu, X. Modulating plant growth−metabolism coordination for sustainable agriculture. *Nature* **2018**, *560* (7720), 595−600.
(41) Wu, K.; Wang, S.; Song, W.; Zhang, J.; Wang, Y.; Liu, Q.; Yu, J.; Ye, Y.; Li, S.; Chen, J.; Zhao, Y.; Wang, J.; Wu, X.; Wang, M.; Zhang, Y.; Liu, B.; Wu, Y.; Harberd, N. P.; Fu, X. Enhanced sustainable green revolution yield via nitrogen-responsive chromatin modulation in rice. *Science* **2020**, *367* (6478), No. eaaz2046.
(42) Huang, Y.; Wang, H.; Zhu, Y.; Huang, X.; Li, S.; Wu, X.; Zhao, Y.; Bao, Z.; Qin, L.; Jin, Y.; Cui, Y.; Ma, G.; Xiao, Q.; Wang, Q.; Wang, J.; Yang, X.; Liu, H.; Lu, X.; Larkins, B. A.; Wang, W.; Wu, Y. THP9 enhances seed protein content and nitrogen-use efficiency in maize. *Nature* **2022**, *612* (7939), 292−300, DOI: 10.1038/s41586-022-05441-2.
(43) Shi, X.; Cui, F.; Han, X.; He, Y.; Zhao, L.; Zhang, N.; Zhu, H.; Liu, Z.; Ma, B.; Zheng, S.; Zhang, W.; Li, J.; Fan, X.; Si, Y.; Tian, S.; Niu, J.; Wu, H.; Liu, X.; Chen, Z.; Meng, D.; et al. Comparative genomic and transcriptomic analyses uncover the molecular basis of high nitrogen-use efficiency in the wheat cultivar Kenong 9204. *Mol. Plant.* **2022**, *15* (9), 1440−1456.
(44) Gregersen, P. L.; Holm, P. B.; Krupinska, K. Leaf senescence and nutrient remobilisation in barley and wheat. *Plant Biol.* **2008**, *10*, 37−49.
(45) Zhang, Z. H.; Zhou, T.; Liao, Q.; Yao, J. Y.; Liang, G. H.; Song, H. X.; Guan, C. Y.; Hua, Y. P. Integrated physiologic, genomic and transcriptomic strategies involving the adaptation of allotetraploid rapeseed to nitrogen limitation. *BMC Plant Biol.* **2018**, *18* (1), 322.
(46) Kong, H.; Landherr, L. L.; Frohlich, M. W.; Leebens-Mack, J.; Ma, H.; dePamphilis, C. W. Patterns of gene duplication in the plant SKP1 gene family in angiosperms: evidence for multiple mechanisms of rapid gene birth. *Plant J.* **2007**, *50*, 873−885.
(47) Orsel, M.; Krapp, A.; Daniel-Vedele, F. Analysis of the NRT2 nitrate transporter family in Arabidopsis. Structure and gene expression. *Plant Physiol.* **2002**, *129* (2), 886−896.
(48) Cai, C.; Wang, J. Y.; Zhu, Y. G.; Shen, Q. R.; Li, B.; Tong, Y. P.; Li, Z. S. Gene structure and expression of the high-affinity nitrate transport system in rice roots. *J. Integr. Plant Biol.* **2008**, *50* (4), 443−451, DOI: 10.1111/j.1744-7909.2008.00642.x.
(49) Liu, W.; Sun, Q.; Wang, K.; Du, Q.; Li, W. X. Nitrogen limitation adaptation (NLA) is involved in source-to-sink remobilization of nitrate by mediating the degradation of NRT1.7 in Arabidopsis. *New Phytol.* **2017**, *214*, 734−744.
(50) Chen, K. E.; Chen, H. Y.; Tseng, C. S.; Tsay, Y. F. Improving nitrogen use efficiency by manipulating nitrate remobilization in plants. *Nat. Plants* **2020**, *6* (9), 1126−1135.
(51) Lin, S. H.; Kuo, H. F.; Canivenc, G.; Lin, C. S.; Lepetit, M.; Hsu, P. K.; Tillard, P.; Lin, H. L.; Wang, Y. Y.; Tsai, C. B.; Gojon, A.; Tsay, Y. F. Mutation of the Arabidopsis NRT1.5 nitrate transporter causes defective root-to-shoot nitrate transport. *Plant Cell* **2008**, *20* (9), 2514−2528.
(52) Zheng, Y.; Drechsler, N.; Rausch, C.; Kunze, R. The Arabidopsis nitrate transporter NPF7.3/NRT1.5 is involved in lateral root development under potassium deprivation. *Plant Signaling Behav.* **2016**, *11* (5), 2832−2847, DOI: 10.1080/15592324.2016.1176819.
(53) Chen, C. Z.; Lv, X. F.; Li, J. Y.; Yi, H. Y.; Gong, J. M. Arabidopsis NRT1.5 is another essential component in the regulation of nitrate reallocation and stress tolerance. *Plant Physiol.* **2012**, *159* (4), 1582−1590.
(54) Watanabe, S.; Takahashi, N.; Kanno, Y.; Suzuki, H.; Aoi, Y.; Takeda-Kamiya, N.; Toyooka, K.; Kasahara, H.; Hayashi, K. I.; Umeda, M.; Seo, M. The Arabidopsis NRT1/PTR FAMILY protein NPF7.3/NRT1.5 is an indole-3-butyric acid transporter involved in root gravitropism. *Proc. Natl. Acad. Sci. U.S.A.* **2020**, *117* (49), 31500−31509.